EUROPEAN ORGANISATION FOR NUCLEAR RESEARCH (CERN)

arXiv:1307.6795v1 [hep-ex] 25 Jul 2013

Dynamics of isolated-photon plus jet production in *pp* collisions at √s = 7 TeV with the ATLAS detector

The ATLAS Collaboration

Abstract

The dynamics of isolated-photon plus jet production in pp collisions at a centre-of-mass energy of 7 TeV has been studied with the ATLAS detector at the LHC using an integrated luminosity of 37 pb^{-1}. Measurements of isolated-photon plus jet bin-averaged cross sections are presented as functions of photon transverse energy, jet transverse momentum and jet rapidity. In addition, the bin-averaged cross sections as functions of the difference between the azimuthal angles of the photon and the jet, the photon–jet invariant mass and the scattering angle in the photon–jet centre-of-mass frame have been measured. Next-to-leading-order QCD calculations are compared to the measurements and provide a good description of the data, except for the case of the azimuthal opening angle.

Dynamics of isolated-photon plus jet production in *pp* collisions at $\sqrt{s} = 7$ TeV with the ATLAS detector

The ATLAS Collaboration

Abstract

The dynamics of isolated-photon plus jet production in *pp* collisions at a centre-of-mass energy of 7 TeV has been studied with the ATLAS detector at the LHC using an integrated luminosity of 37 pb^{-1}. Measurements of isolated-photon plus jet bin-averaged cross sections are presented as functions of photon transverse energy, jet transverse momentum and jet rapidity. In addition, the bin-averaged cross sections as functions of the difference between the azimuthal angles of the photon and the jet, the photon–jet invariant mass and the scattering angle in the photon–jet centre-of-mass frame have been measured. Next-to-leading-order QCD calculations are compared to the measurements and provide a good description of the data, except for the case of the azimuthal opening angle.

Keywords: QCD, photon, jet

1. Introduction

The production of prompt photons in association with a jet in proton–proton collisions, $pp \rightarrow \gamma$+jet+X, provides a testing ground for perturbative QCD (pQCD) in a cleaner environment than in jet production, since the photon originates directly from the hard interaction. The measurements of angular correlations between the photon and the jet can be used to probe the dynamics of the hard-scattering process. Since the dominant production mechanism in *pp* collisions at the LHC is through the $qg \rightarrow q\gamma$ process, measurements of prompt-photon plus jet production have been used to constrain the gluon density in the proton [1, 2]. Furthermore, precise measurements of photon plus jet production are also useful for the tuning of the Monte Carlo (MC) models. In addition, these events constitute the main reducible background in the identification of Higgs bosons decaying to a photon pair.

The dynamics of the underlying processes in $2 \rightarrow 2$ hard collinear scattering can be investigated using the variable θ^*, where $\cos\theta^* \equiv \tanh(\Delta y/2)$ and Δy is the difference between the rapidities[1] of the two final-state particles. The variable θ^* coincides with the scattering angle in

---

[1] The ATLAS reference system is a Cartesian right-handed coordinate system, with the nominal collision point at the origin. The anticlockwise beam direction defines the positive *z*-axis, while the positive *x*-axis is defined as pointing from the collision point to the centre of the LHC ring and the positive *y*-axis points upwards. The azimuthal angle ϕ is measured around the beam axis, and the polar angle θ is measured with respect to the *z*-axis. Pseudorapidity is defined as $\eta = -\ln\tan(\theta/2)$, rapidity is defined as $y = 0.5\ln[(E + p_z)/(E - p_z)]$, where E is the energy and p_z is the *z*-component of the momentum, and transverse energy is defined as $E_T = E \sin\theta$.

the centre-of-mass frame, and its distribution is sensitive to the spin of the exchanged particle. For processes dominated by t-channel gluon exchange, such as dijet production in pp collisions shown in Fig. 1(a), the differential cross section behaves as $(1 - |\cos\theta^*|)^{-2}$ when $|\cos\theta^*| \to 1$. In contrast, processes dominated by t-channel quark exchange, such as W/Z + jet production shown in Fig. 1(b), are expected to have an asymptotic $(1 - |\cos\theta^*|)^{-1}$ behaviour. This fundamental prediction of QCD can be tested in photon plus jet production at the centre-of-mass energy of the LHC.

At leading order (LO) in pQCD, the process $pp \to \gamma$ + jet + X proceeds via two production mechanisms: direct photons (DP), which originate from the hard process, and fragmentation photons (F), which arise from the fragmentation of a coloured high transverse momentum (p_T) parton [3, 4]. The direct-photon contribution, as shown in Fig. 1(c), is expected to exhibit a $(1 - |\cos\theta^*|)^{-1}$ dependence when $|\cos\theta^*| \to 1$, whereas that of fragmentation processes, as shown in Fig. 1(d), is predicted to be the same as in dijet production, namely $(1 - |\cos\theta^*|)^{-2}$. For both processes, there are also s-channel contributions which are, however, non-singular when $|\cos\theta^*| \to 1$. As a result, a measurement of the cross section for prompt-photon plus jet production as a function of $|\cos\theta^*|$ provides a handle on the relative contributions of the direct-photon and fragmentation components as well as the possibility to test the dominance of t-channel quark exchange, such as that shown in Fig. 1(c).
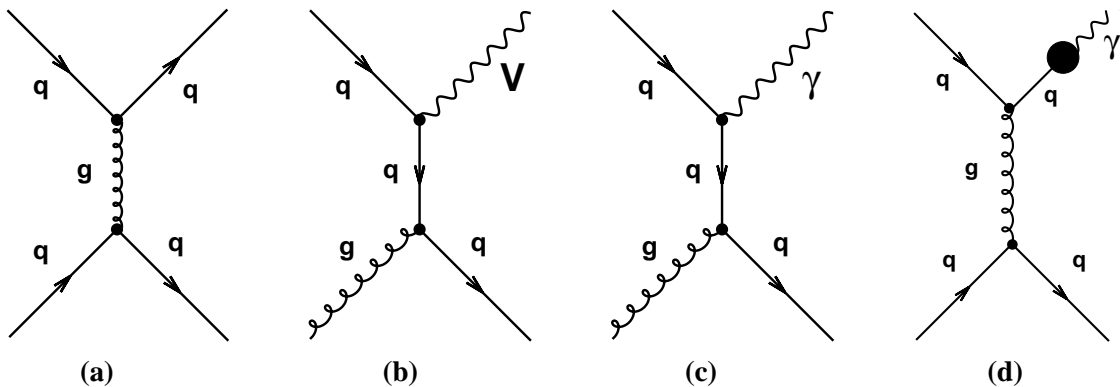

Figure 1: Examples of Feynman diagrams for (a) dijet production, (b) V + jet production with $V = W$ or Z, (c) γ + jet production through direct-photon processes and (d) γ + jet production through fragmentation processes.

Measurements of prompt-photon production in a final state with accompanying hadrons necessitates of an isolation requirement on the photon to avoid the large contribution from neutral-hadron decays into photons. The production of inclusive isolated photons in pp collisions has been studied previously by ATLAS [5, 6] and CMS [7, 8]. Recently, the differential cross sections for isolated photons in association with jets as functions of the photon transverse energy in different regions of rapidity of the highest transverse-momentum (leading) jet were measured by ATLAS [9]. The analysis presented in this paper is based on the same data sample and similar selection criteria as in the previous publication, but extends the study by measuring also cross sections in terms of the leading-jet and photon-plus-jet properties. The goal of the analysis presented here is to study the kinematics and dynamics of the isolated-photon plus jet system by measur-

2

ing the bin-averaged cross sections as functions of the leading-photon transverse energy (E_T^γ), the leading-jet transverse momentum (p_T^{jet}) and rapidity (y^{jet}), the difference between the azimuthal angles of the photon and the jet ($\Delta\phi^{\gamma j}$), the photon–jet invariant mass ($m^{\gamma j}$) and $\cos\theta^{\gamma j}$, where the variable θ^* is referred to as $\theta^{\gamma j}$ here and henceforth. The photon was required to be isolated by using the same isolation criterion as in previous measurements [5, 6, 9] based on the amount of transverse energy inside the cone given by $\sqrt{(\eta - \eta^\gamma)^2 + (\phi - \phi^\gamma)^2} \leq \Delta R = 0.4$, centred around the photon direction (defined by η^γ and ϕ^γ). The jets were defined using the anti-k_t jet algorithm [10] with distance parameter $R = 0.6$. The measurements were performed in the phase-space region of $E_T^\gamma > 45$ GeV, $|\eta^\gamma| < 2.37$ (excluding the region $1.37 < |\eta^\gamma| < 1.52$), $p_T^{\text{jet}} > 40$ GeV, $|y^{\text{jet}}| < 2.37$ and $\Delta R_{\gamma j}^2 = (\eta^\gamma - \eta^{\text{jet}})^2 + (\phi^\gamma - \phi^{\text{jet}})^2 > 1$. The measurements of $d\sigma/dm^{\gamma j}$ and $d\sigma/d|\cos\theta^{\gamma j}|$ were performed for $|\eta^\gamma + y^{\text{jet}}| < 2.37$, $|\cos\theta^{\gamma j}| < 0.83$ and $m^{\gamma j} > 161$ GeV; these additional requirements select a region where the $m^{\gamma j}$ and $|\cos\theta^{\gamma j}|$ distributions are not distorted by the restrictions on the transverse momenta and rapidities of the photon and the jet. Next-to-leading-order (NLO) QCD calculations were compared to the measurements. Photon plus jet events constitute an important background in the identification of the Higgs decaying into diphotons; the $|\cos\theta^*|$ distribution for the diphoton events has been used [11] to study the spin of the new "Higgs-like" particle observed by ATLAS [12] and CMS [13]. To understand the photon plus jet background in terms of pQCD and to aid in better constraining the contributions of direct-photon and fragmentation processes in the MC models, a measurement of the bin-averaged cross section as a function of $|\cos\theta^{\gamma j}|$ was also performed without the restrictions on $m^{\gamma j}$ or on $|\eta^\gamma + y^{\text{jet}}|$. Predictions from both leading-logarithm parton-shower MC models and NLO QCD calculations were compared to this measurement.

2. The ATLAS detector

The ATLAS experiment [14] uses a multi-purpose particle detector with a forward-backward symmetric cylindrical geometry and nearly 4π coverage in solid angle.

The inner detector covers the pseudorapidity range $|\eta| < 2.5$ and consists of a silicon pixel detector, a silicon microstrip detector and, for $|\eta| < 2$, a transition radiation tracker. The inner detector is surrounded by a thin superconducting solenoid providing a 2 T magnetic field and is used to measure the momentum of charged-particle tracks.

The electromagnetic calorimeter is a lead liquid-argon (LAr) sampling calorimeter. It is divided into a barrel section, covering the pseudorapidity region $|\eta| < 1.475$, and two end-cap sections, covering the pseudorapidity regions $1.375 < |\eta| < 3.2$. It consists of three shower-depth layers in most of the pseudorapidity range. The first layer is segmented into narrow strips in the η direction (width between 0.003 and 0.006 depending on η, with the exception of the regions $1.4 < |\eta| < 1.5$ and $|\eta| > 2.4$). This high granularity provides discrimination between single-photon showers and two overlapping showers coming from, for example, a π^0 decay. The second layer of the electromagnetic calorimeter, which collects most of the energy deposited in the calorimeter by the photon shower, has a cell granularity of 0.025×0.025 in $\eta \times \phi$. A third layer collects the tails of the electromagnetic showers. An additional thin LAr presampler covers $|\eta| < 1.8$ to correct for energy loss in material in front of the calorimeter. The electromagnetic energy scale is calibrated using $Z \rightarrow ee$ events with an uncertainty less than 1% [15].

A hadronic sampling calorimeter is located outside the electromagnetic calorimeter. It is made of scintillator tiles and steel in the barrel section ($|\eta| < 1.7$) and of two end-caps of copper and LAr ($1.5 < |\eta| < 3.2$). The forward region ($3.1 < |\eta| < 4.9$) is instrumented with a copper/tungsten LAr calorimeter for both electromagnetic and hadronic measurements. Outside the ATLAS calorimeters lies the muon spectrometer, which identifies and measures the deflection of muons up to $|\eta| = 2.7$, in a magnetic field generated by superconducting air-core toroidal magnet systems.

Events containing photon candidates were selected by a three-level trigger system. The first-level trigger (level-1) is hardware-based and uses a trigger cell granularity of 0.1×0.1 in $\eta \times \phi$. The algorithms of the second- and third-level triggers are implemented in software and exploit the full granularity and precision of the calorimeter to refine the level-1 trigger selection, based on improved energy resolution and detailed information on energy deposition in the calorimeter cells.

3. Data selection

The data used in this analysis were collected during the proton–proton collision running period of 2010, when the LHC operated at a centre-of-mass energy of $\sqrt{s} = 7$ TeV. This data set was chosen to study the dynamics of isolated-photon plus jet production down to $E_T^\gamma = 45$ GeV.

Only events taken in stable beam conditions and passing detector and data-quality requirements were considered. Events were recorded using a single-photon trigger, with a nominal transverse energy threshold of 40 GeV; this trigger was used to collect events in which the photon transverse energy, after reconstruction and calibration, was greater than 45 GeV. The total integrated luminosity of the collected sample amounts to 37.1 ± 1.3 pb^{-1} [16].

The selection criteria applied by the trigger to shower-shape variables computed from the energy profiles of the showers in the calorimeters are looser than the photon identification criteria applied in the offline analysis; for isolated photons with $E_T^\gamma > 43$ GeV and pseudorapidity $|\eta^\gamma| < 2.37$, the trigger efficiency is close to 100%.

The sample of isolated-photon plus jet events was selected using offline criteria similar to those reported in the previous publication [9] and described below.

Events were required to have a reconstructed primary vertex, with at least five associated charged-particle tracks with $p_T > 150$ MeV, consistent with the average beam-spot position. This requirement reduced non-collision backgrounds. The effect of this requirement on the signal was found to be negligible. The remaining fraction of non-collision backgrounds was estimated to be less than 0.1% [5, 6].

During the 2010 data-taking period, there were on average 2–3 proton–proton interactions per bunch crossing. The effects of the additional pp interactions (pile-up) on the photon isolation and jet reconstruction are described below.

3.1. Photon selection

The selection of photon candidates is based on the reconstruction of isolated electromagnetic clusters in the calorimeter with transverse energies exceeding 2.5 GeV. Clusters were matched to charged-particle tracks based on the distance in (η, ϕ) between the cluster centre and the track impact point extrapolated to the second layer of the LAr calorimeter. Clusters matched to tracks were classified as electron candidates, whereas those without matching tracks were classified as

unconverted photon candidates. Clusters matched to pairs of tracks originating from reconstructed conversion vertices in the inner detector or to single tracks with no hit in the innermost layer of the pixel detector were classified as converted photon candidates [17]. The overall reconstruction efficiency for unconverted (converted) photons with transverse energy above 20 GeV and pseudorapidity in the range $|\eta^\gamma| < 2.37$, excluding the transition region $1.37 < |\eta^\gamma| < 1.52$ between calorimeter sections, was estimated to be 99.8 (94.3)% [17]. The final energy measurement, for both converted and unconverted photons, was made using only the calorimeter, with a cluster size depending on the photon classification. In the barrel, a cluster corresponding to 3×5 ($\eta \times \phi$) cells in the second layer was used for unconverted photons, while a cluster of 3×7 cells was used for converted photon candidates to compensate for the opening angle between the conversion products in the ϕ direction due to the magnetic field. In the end-cap, a cluster size of 5×5 was used for all candidates. A dedicated energy calibration [18] was then applied separately for converted and unconverted photon candidates to account for upstream energy loss and both lateral and longitudinal leakage. Photons reconstructed near regions of the calorimeter affected by readout or high-voltage failures were rejected, eliminating around 5% of the selected candidates.

Events with at least one photon candidate with calibrated $E_T^\gamma > 45$ GeV and $|\eta^\gamma| < 2.37$ were selected. The candidate was excluded if $1.37 < |\eta^\gamma| < 1.52$. The same shower-shape and isolation requirements as described in previous publications [5, 6, 9] were applied to the candidates; these requirements are referred to as "tight" identification criteria. The selection criteria for the shower-shape variables are independent of the photon-candidate transverse energy, but vary as a function of the photon pseudorapidity, to take into account significant changes in the total thickness of the upstream material and variations in the calorimeter geometry or granularity. They were optimised independently for unconverted and converted photons to account for the different developments of the showers in each case. The application of these selection criteria suppresses background from jets misidentified as photons.

The photon candidate was required to be isolated by restricting the amount of transverse energy around its direction. The transverse energy deposited in the calorimeters inside a cone of radius $\Delta R = 0.4$ centred around the photon direction is denoted by $E_{T,det}^{iso}$. The contributions from those cells (in any layer) in a window corresponding to 5×7 cells of the second layer of the electromagnetic calorimeter around the photon-shower barycentre are not included in the sum. The mean value of the small leakage of the photon energy outside this region, evaluated as a function of the photon transverse energy, was subtracted from the measured value of $E_{T,det}^{iso}$. The typical size of this correction is a few percent of the photon transverse energy. The measured value of $E_{T,det}^{iso}$ was further corrected by subtracting the estimated contributions from the underlying event and additional inelastic pp interactions. This correction was computed on an event-by-event basis and amounted on average to 900 MeV [6]. After all these corrections, $E_{T,det}^{iso}$ was required to be below 3 GeV for a photon to be considered isolated.

The relative contribution to the total cross section from fragmentation processes decreases after the application of this requirement, though it remains non-negligible especially at low transverse energies. The isolation requirement significantly reduces the main background, which consists of multi-jet events where one jet typically contains a π^0 or η meson that carries most of the jet energy and is misidentified as an isolated photon because it decays into an almost collinear photon pair.

A small fraction of events contain more than one photon candidate passing the selection crite-

ria. In such events, the highest-E_T^γ (leading) photon was kept for further study.

3.2. Jet selection

Jets were reconstructed from three-dimensional topological clusters built from calorimeter cells, using the anti-k_t algorithm with distance parameter $R = 0.6$. The jet four-momenta were computed from the sum of the topological cluster four-momenta, treating each as a four-vector with zero mass. The jet four-momenta were then recalibrated using a jet energy scale (JES) correction described in Ref. [19]. This calibration procedure corrected the jets for calorimeter instrumental effects, such as inactive material and noncompensation, as well as for the additional energy due to multiple pp interactions within the same bunch crossing. These jets are referred to as detector-level jets. The uncertainty on the JES correction in the central (forward) region, $|\eta| < 0.8$ ($2.1 < |\eta| < 2.8$), is less than 4.6% (6.5%) for all jets with transverse momentum $p_T > 20$ GeV and less than 2.5% (3%) for jets with $60 < p_T < 800$ GeV.

Jets reconstructed from calorimeter signals not originating from a pp collision were rejected by applying jet-quality criteria [19]. These criteria suppressed fake jets from electronic noise in the calorimeter, cosmic rays and beam-related backgrounds. Remaining jets were required to have calibrated transverse momenta greater than 40 GeV. Jets overlapping with the candidate photon or with an isolated electron were discarded; if the jet axis lay within a cone of radius $\Delta R = 1$ (0.3) around the leading-photon (isolated-electron) candidate, the jet was discarded. The removal of electrons misidentified as jets suppresses contamination from W/Z plus jet events. In events with multiple jets satisfying the above requirements, the jet with highest p_T^{jet} (leading jet) was retained for further study. The leading-jet rapidity was required to be in the region $|y^{\text{jet}}| < 2.37$.

3.3. Final photon plus jet sample

The above requirements select approximately 124 000 events. The fraction of events with multiple photons fulfilling the above conditions is $3 \cdot 10^{-4}$. The average jet multiplicity in the data is 1.19. The signal MC (see Section 4) predictions for the jet multiplicity are 1.21 in PYTHIA [20] and 1.19 in HERWIG [21].

For the measurements of the bin-averaged cross sections as functions of $m^{\gamma\text{j}}$ and $|\cos\theta^{\gamma\text{j}}|$, additional requirements were imposed to remove the bias due to the rapidity and transverse-momentum requirements on the photon and the jet. Specifically, to have a uniform coverage in both $\cos\theta^{\gamma\text{j}}$ and $m^{\gamma\text{j}}$, the restrictions $|\eta^\gamma + y^{\text{jet}}| < 2.37$, $|\cos\theta^{\gamma\text{j}}| < 0.83$ and $m^{\gamma\text{j}} > 161$ GeV were applied. The first two requirements restrict the phase space to the inside of the square delineated by the dashed lines, as shown in Fig. 2(a); within this square, slices in $\cos\theta^{\gamma\text{j}}$ have the same length along the $\eta^\gamma + y^{\text{jet}}$ axis. The third requirement avoids the bias induced by the minimal requirement on E_T^γ, as shown in Fig.2(b); the hatched area represents the largest region in which unbiased measurements of both $|\cos\theta^{\gamma\text{j}}|$ and $m^{\gamma\text{j}}$ distributions can be performed. These requirements do not remove the small bias due to the exclusion of the $1.37 < |\eta^\gamma| < 1.52$ region. The number of events selected in the data after these additional requirements is approximately 26 000.

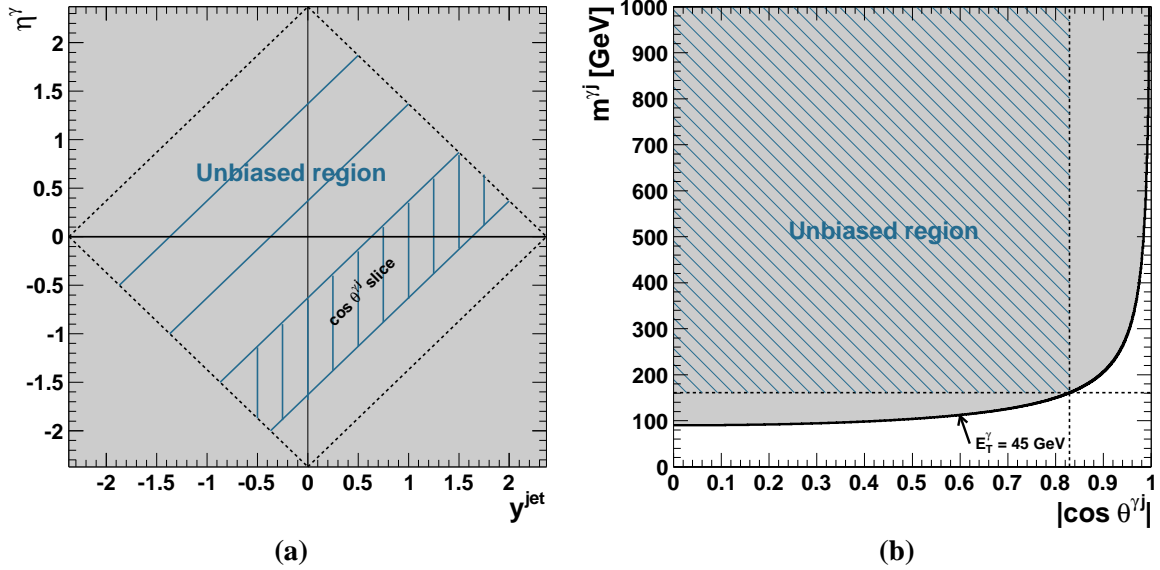The contamination from jets produced in pile-up events in the selected samples was estimated to be negligible.

Figure 2: The selected regions in the (a) η^γ-y^{jet} and (b) $m^{\gamma\text{j}}$-$|\cos\theta^{\gamma\text{j}}|$ planes. In (a), the dashed lines correspond to: $\eta^\gamma + y^{\text{jet}} = 2.37$ (first quadrant), $\eta^\gamma - y^{\text{jet}} = 2.37$ (second quadrant), $\eta^\gamma + y^{\text{jet}} = -2.37$ (third quadrant) and $\eta^\gamma - y^{\text{jet}} = -2.37$ (fourth quadrant). In (b), the horizontal (vertical) dashed line corresponds to $m^{\gamma\text{j}} = 161$ GeV ($|\cos\theta^{\gamma\text{j}}| = 0.83$) and the solid line corresponds to $E_{\text{T}}^\gamma = 45$ GeV.

4. Monte Carlo simulations

Samples of simulated events were generated to study the characteristics of signal and background. These MC samples were also used to determine the response of the detector to jets of hadrons and the correction factors necessary to obtain the particle-level cross sections. In addition, they were used to estimate hadronisation corrections to the NLO QCD calculations.

The MC programs Pythia 6.423 [20] and Herwig 6.510 [21] were used to generate the simulated signal events. In both generators, the partonic processes are simulated using leading-order matrix elements, with the inclusion of initial- and final-state parton showers. Fragmentation into hadrons was performed using the Lund string model [22] in the case of Pythia and the cluster model [23] in the case of Herwig. The modified leading-order MRST2007 [24, 25] parton distribution functions (PDFs) were used to parameterise the proton structure. Both samples include a simulation of the underlying event, via the multiple-parton interaction model in the case of Pythia and via the Jimmy package [26] in the case of Herwig. The event-generator parameters, including those of the underlying-event modelling, were set according to the AMBT1 [27] and AUET1 [28] tunes for Pythia and Herwig, respectively. All the samples of generated events were passed through the Geant4-based [29] ATLAS detector simulation program [30]. They were reconstructed and analysed by the same program chain as the data.

The Pythia simulation of the signal includes leading-order photon plus jet events from both direct processes (the hard subprocesses $qg \rightarrow q\gamma$ and $q\bar{q} \rightarrow g\gamma$) and photon bremsstrahlung in QCD dijet events, which can be generated simultaneously. On the other hand, the Herwig signal sample was obtained from the cross-section-weighted mixture of samples containing only direct-

photon plus jet or only bremsstrahlung-photon plus jet events, since these processes cannot be generated simultaneously.

The multi-jet background was simulated by using all tree-level $2 \rightarrow 2$ QCD processes and removing photon plus jet events from photon bremsstrahlung. The background from diphoton events was estimated using Pythia MC samples by computing the ratio of diphoton to isolated-photon plus jet events and was found to be negligible [9].

Particle-level jets in the MC simulation were reconstructed using the anti-k_t jet algorithm and were built from stable particles, which are defined as those with a rest-frame lifetime longer than 10 ps. The particle-level isolation requirement on the photon was applied to the transverse energy of all stable particles, except for muons and neutrinos, in a cone of radius $\Delta R = 0.4$ around the photon direction after the contribution from the underlying event was subtracted; in this case, the same underlying-event subtraction procedure used on data was applied at the particle level. The isolation transverse energy at particle level is denoted by $E_{\mathrm{T,part}}^{\mathrm{iso}}$. The measured bin-averaged cross sections refer to particle-level jets and photons that are isolated by requiring $E_{\mathrm{T,part}}^{\mathrm{iso}} < 4$ GeV [5].

For the comparison to the measurements (see Section 9), samples of events were generated at the particle level using the Sherpa 1.3.1 [31] program interfaced with the CTEQ6L1 [32] PDF set. The samples were generated with LO matrix elements for photon plus jet final states with up to three additional partons, supplemented with parton showers. Fragmentation into hadrons was performed using a modified version of the cluster model [33].

5. Signal extraction

5.1. Background subtraction and signal-yield estimation

A non-negligible background contribution remains in the selected sample, even after the application of the tight identification and isolation requirements on the photon. This background comes predominantly from multi-jet processes, in which a jet is misidentified as a photon. This jet usually contains a light neutral meson, mostly a π^0 decaying into two collimated photons, which carries most of the jet energy. The very small contributions expected from diphoton and W/Z plus jet events [5, 9] are neglected.

The background subtraction does not rely on MC background samples but uses instead a data-driven method based on signal-depleted control regions. The background contamination in the selected sample was estimated using the same two-dimensional sideband technique as in the previous analyses [5, 6, 9] and then subtracted bin-by-bin from the observed yield. In this method, the photon was classified as:

- "isolated", if $E_{\mathrm{T,det}}^{\mathrm{iso}} < 3$ GeV;

- "non-isolated", if $E_{\mathrm{T,det}}^{\mathrm{iso}} > 5$ GeV;

- "tight", if it passed the tight photon identification criteria;

- "non-tight", if it failed at least one of the tight requirements on the shower-shape variables computed from the energy deposits in the first layer of the electromagnetic calorimeter, but passed all the other tight identification criteria.

In the two-dimensional plane formed by $E_{\mathrm{T,det}}^{\mathrm{iso}}$ and the photon identification variable, four regions were defined:

- A: the "signal" region, containing tight and isolated photon candidates;

- B: the "non-isolated" background control region, containing tight and non-isolated photon candidates;

- C: the "non-identified" background control region, containing isolated and non-tight photon candidates;

- D: the background control region containing non-isolated and non-tight photon candidates.

The signal yield in region A, N_A^{sig}, was estimated by using the relation

$$
N_A^{\mathrm{sig}} = N_A - R^{\mathrm{bg}} \cdot (N_B - \epsilon_B N_A^{\mathrm{sig}}) \cdot \frac{(N_C - \epsilon_C N_A^{\mathrm{sig}})}{(N_D - \epsilon_D N_A^{\mathrm{sig}})}, \tag{1}
$$

where N_K, with $K = A, B, C, D$, is the number of events observed in region K and

$$
R^{\mathrm{bg}} = \frac{N_A^{\mathrm{bg}} \cdot N_D^{\mathrm{bg}}}{N_B^{\mathrm{bg}} \cdot N_C^{\mathrm{bg}}}
$$

is the so-called background correlation and was taken as $R^{\mathrm{bg}} = 1$ for the nominal results; N_K^{bg} with $K = A, B, C, D$ is the number of background events in each region. Eq. (1) takes into account the expected number of signal events in the three background control regions (N_K^{sig}) via the signal leakage fractions, $\epsilon_K = N_K^{\mathrm{sig}}/N_A^{\mathrm{sig}}$ with $K = B, C, D$, which were extracted from MC simulations of the signal. Since the simulation does not accurately describe the electromagnetic shower profiles, a correction factor for each simulated shape variable was applied to better match the data [5, 6]. Eq. (1) leads to a second-order polynomial equation in N_A^{sig} that has only one physical ($N_A^{\mathrm{sig}} > 0$) solution.

This method was tested on a cross section-weighted combination of simulated signal and background samples and found to accurately determine the amount of signal in the mixture. The only hypothesis underlying Eq. (1) is that the isolation and identification variables are uncorrelated in background events, thus $R^{\mathrm{bg}} = 1$. This assumption was verified both in simulated background samples and in data in the background-dominated region defined by $E_{\mathrm{T,det}}^{\mathrm{iso}} > 10$ GeV. Deviations from unity were taken as systematic uncertainties (see Section 7).

The signal purity, defined as N_A^{sig}/N_A, is typically above 0.9 and is similar whether PYTHIA or HERWIG is used to extract the signal leakage fractions. The signal purity increases as E_{T}^{γ}, $p_{\mathrm{T}}^{\mathrm{jet}}$ and $m^{\gamma\mathrm{j}}$ increase, is approximately constant as a function of $|y^{\mathrm{jet}}|$ and $\Delta\phi^{\gamma\mathrm{j}}$ and decreases as $|\cos\theta^{\gamma\mathrm{j}}|$ increases.

The signal yield in data and the predictions of the signal MC simulations are compared in Figs. 3–5. Both PYTHIA and HERWIG give an adequate description of the E_{T}^{γ}, $|y^{\mathrm{jet}}|$ and $m^{\gamma\mathrm{j}}$ data distributions. The measured $p_{\mathrm{T}}^{\mathrm{jet}}$ distribution is described well for $p_{\mathrm{T}}^{\mathrm{jet}} \lesssim 100$ GeV; for $p_{\mathrm{T}}^{\mathrm{jet}} \gtrsim 100$ GeV, the simulation of PYTHIA (HERWIG) has a tendency to be somewhat above (below) the data.

9

The simulation of Pythia provides an adequate description of the $\Delta\phi^{\gamma j}$ data distribution, whereas that of Herwig is somewhat poorer. The $|\cos\theta^{\gamma j}|$ data distribution, with or without additional requirements on $m^{\gamma j}$ or $|\eta^{\gamma} + y^{jet}|$, is not well described by either Pythia or Herwig.

For most of these distributions, the shapes of the direct-photon and fragmentation components in the signal MC simulations are somewhat different. Therefore, in each case, the shape of the total MC distribution depends on the relative fraction of the two contributions. To obtain an improved description of the data by the leading-order plus parton-shower MC samples, a fit to each data distribution[2] was performed with the weight of the direct-photon contribution, α, as the free parameter; the weight of the fragmentation contribution was given by $1 - \alpha$. In this context, the default admixture used in the MC simulations would be represented by $\alpha = 0.5$. The fitted values of α were found to be different for each observable and in the range 0.26–0.84. It is emphasized that α does not represent a physical observable and it was used solely for the purpose of improving the description of the data by the LO simulations. Nevertheless, an observable-dependent α may approximate the effects of higher-order terms.[3]

After adjusting the fractions of the DP and F components separately for each distribution, a good description of the data was obtained by both the Pythia and Herwig MC simulations for all the observables (see Figs. 6–8), though the descriptions of $\Delta\phi^{\gamma j}$ and p_T^{jet} by Herwig are still somewhat poor. The MC simulations using the optimised admixture for each observable were used as the baseline for the determination of the measured cross sections (see Section 6).

To be consistent, the optimisation of the admixture of the two components should be done simultaneously with the background subtraction since the signal leakage fractions ϵ_K also depend on the admixture. However, such a procedure would result in an estimated signal yield that would depend on the fitted variable. To obtain a signal yield independent of the observable, except for statistical fluctuations, the background subtraction was performed using the default admixture of the two components and a systematic uncertainty on the background subtraction due to this admixture was included (see Section 7).

5.2. Signal efficiency

The total selection efficiency, including trigger, reconstruction, particle identification and event selection, was evaluated from the simulated signal samples described in Section 4. The integrated efficiency was computed as $\varepsilon = N^{det,part}/N^{part}$, where $N^{det,part}$ is the number of MC events that pass all the selection requirements at both the detector and particle levels and N^{part} is the number of MC events that pass the selection requirements at the particle level. The integrated efficiency was found to be 68.5 (67.9)% from the Pythia (Herwig) samples. The bin-to-bin efficiency was computed as $\varepsilon_i = N_i^{det,part}/N_i^{part}$, where $N_i^{det,part}$ is the number of MC events that pass all the selection requirements at both the detector and particle levels and are generated and reconstructed in bin i,

---

[2] For the distribution of y^{jet}, the result of the fit to that of p_T^{jet} was used.

[3] In Pythia and Herwig, the two components are simulated to LO. The NLO QCD radiative corrections are expected to affect differently the two components and their entanglement, making any distinction impossible. In fact, a variation was observed in the application of the same procedure at parton level: the optimal value of α resulting from a fit of the parton-level predictions of the two components in either Pythia or Herwig to the NLO QCD calculations (see Section 8) depended on the observable.
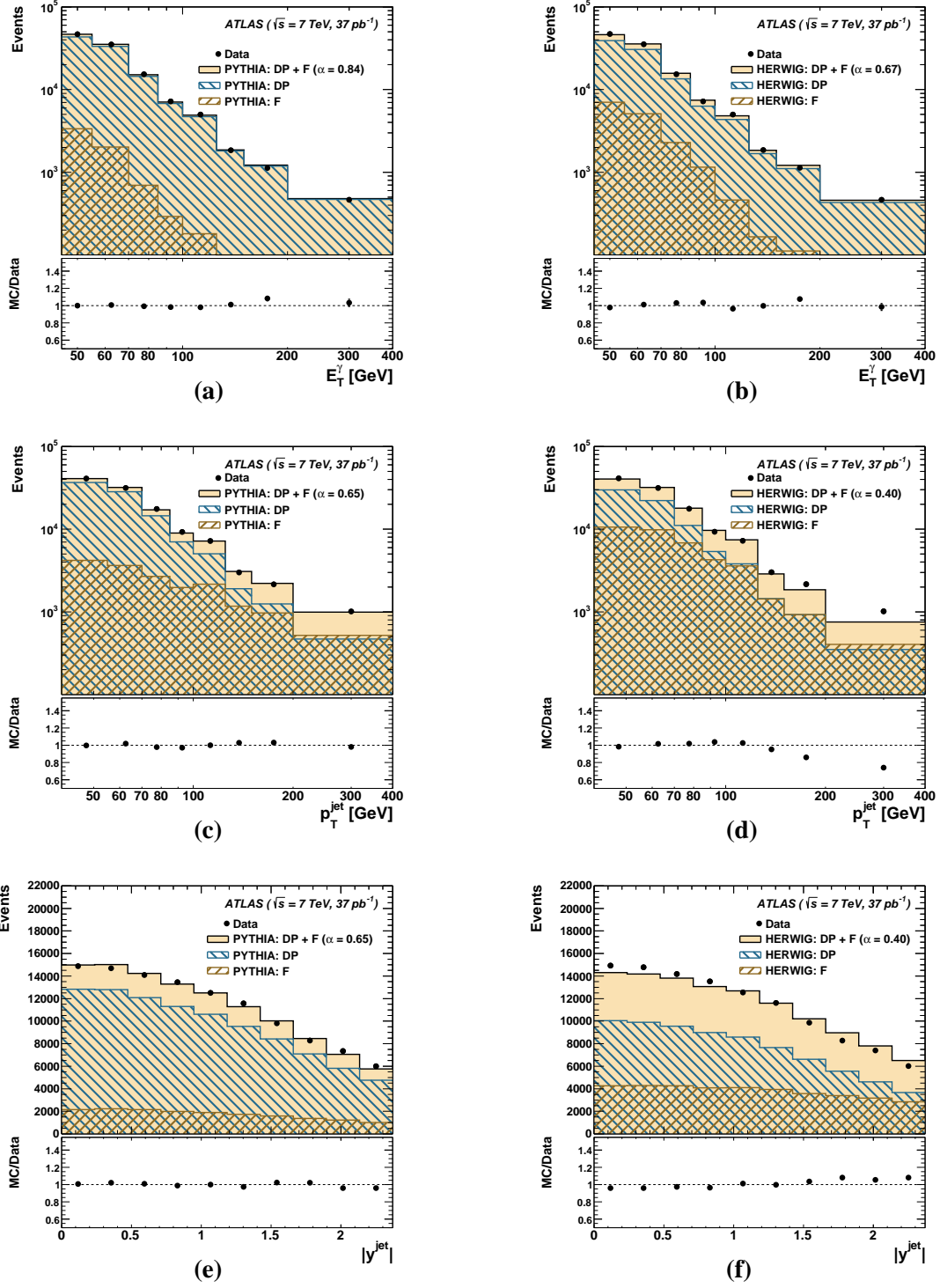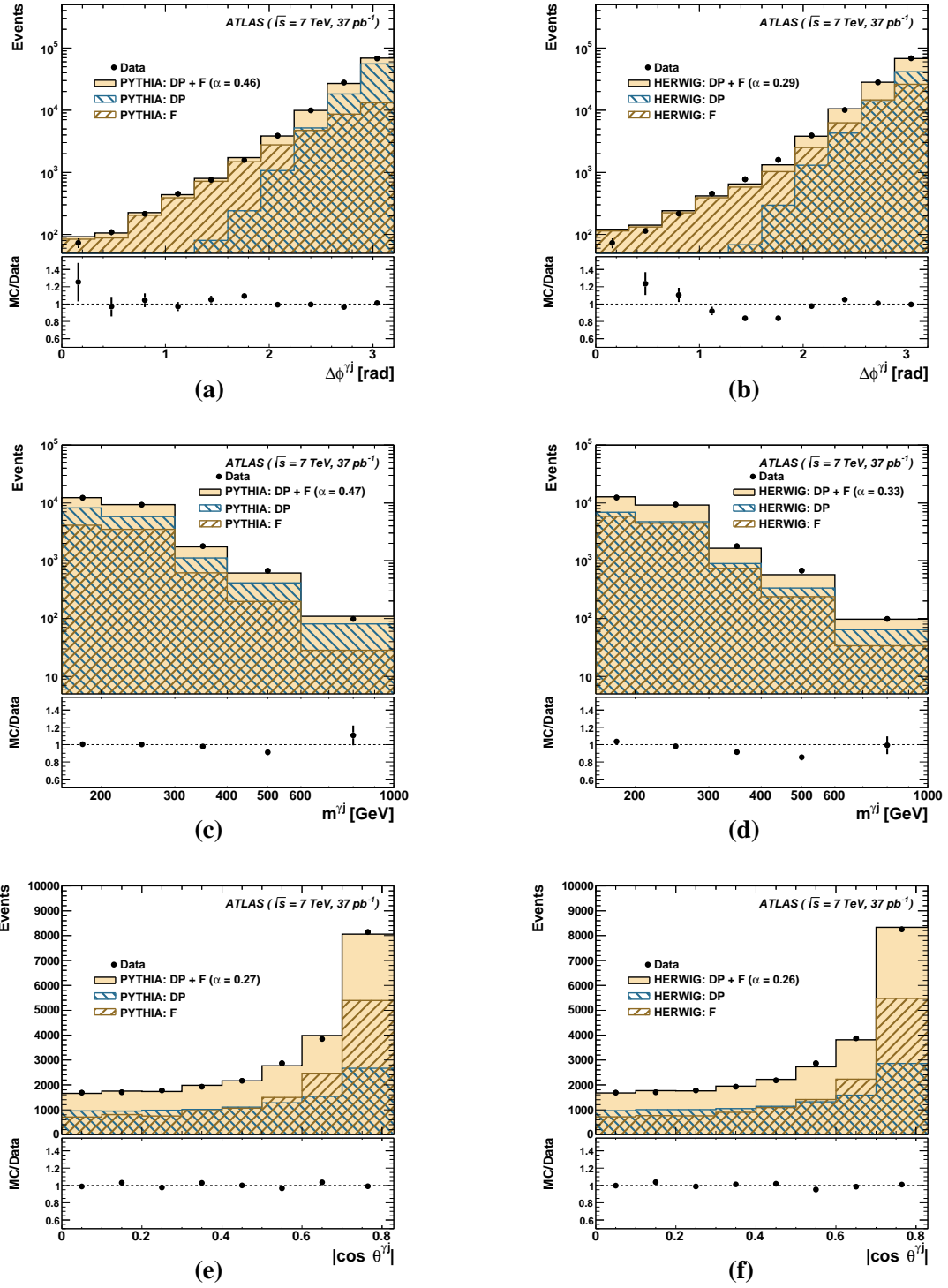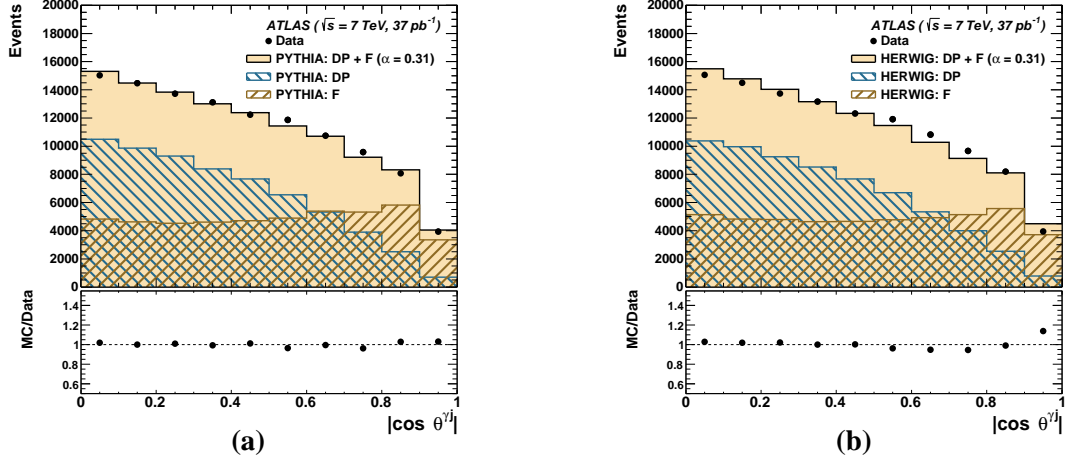
10
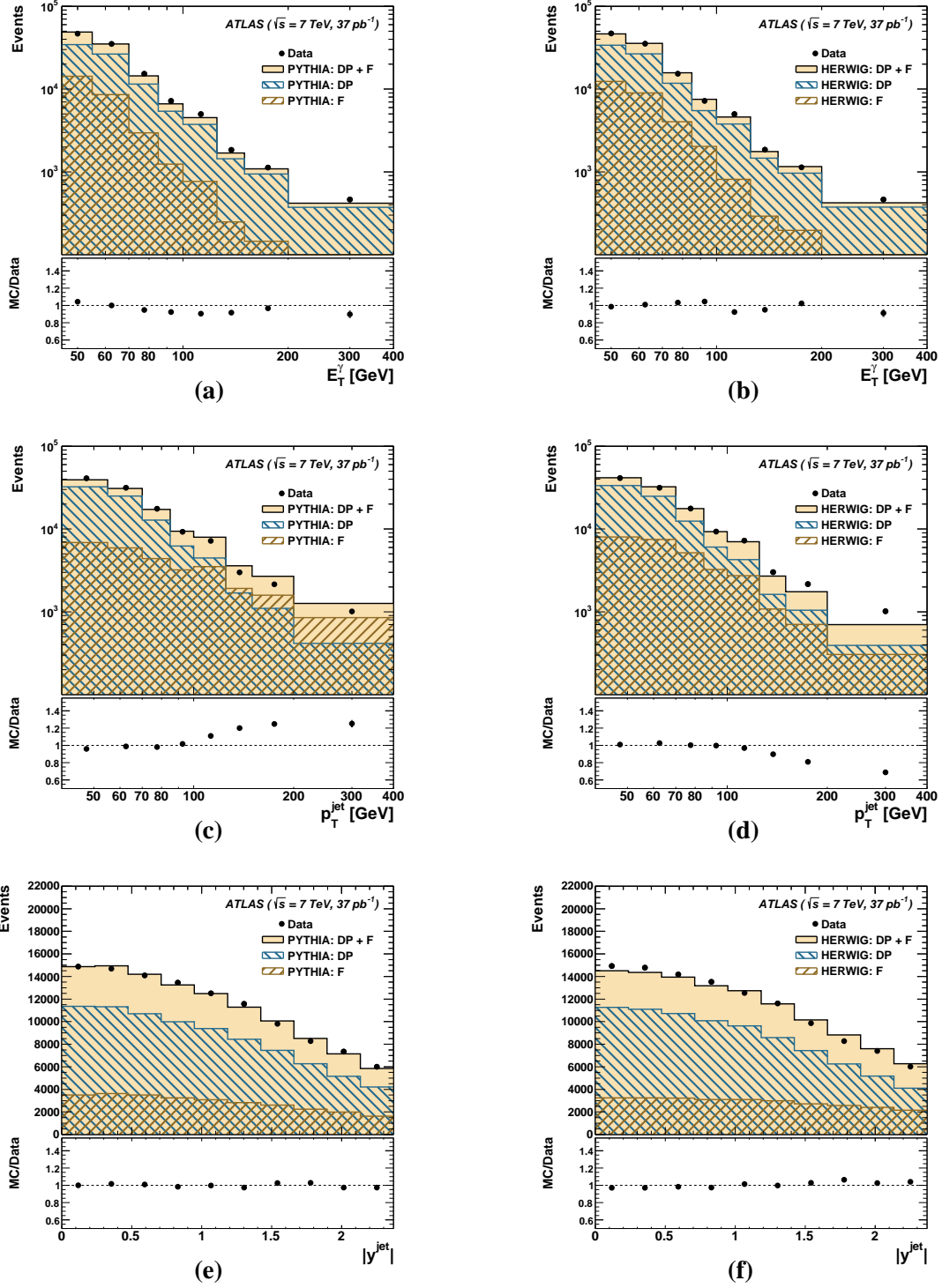
Figure 3: The estimated signal yield in data (dots) using the signal leakage fractions from (a,c,e) Pythia or (b,d,f) Herwig as functions of (a,b) E_T^γ, (c,d) p_T^{jet} and (e,f) $|y^{jet}|$. The error bars represent the statistical uncertainties that, for most of the points, are smaller than the marker size and, thus, not visible. For comparison, the MC simulations of the signal from Pythia and Herwig (shaded histograms) are also included in (a,c,e) and (b,d,f), respectively. The MC distributions are normalised to the total number of data events. The direct-photon (DP, right-hatched histograms) and fragmentation (F, left-hatched histograms) components of the MC simulations are also shown. The ratio of the MC predictions to the data are shown in the bottom part of the figures.

11
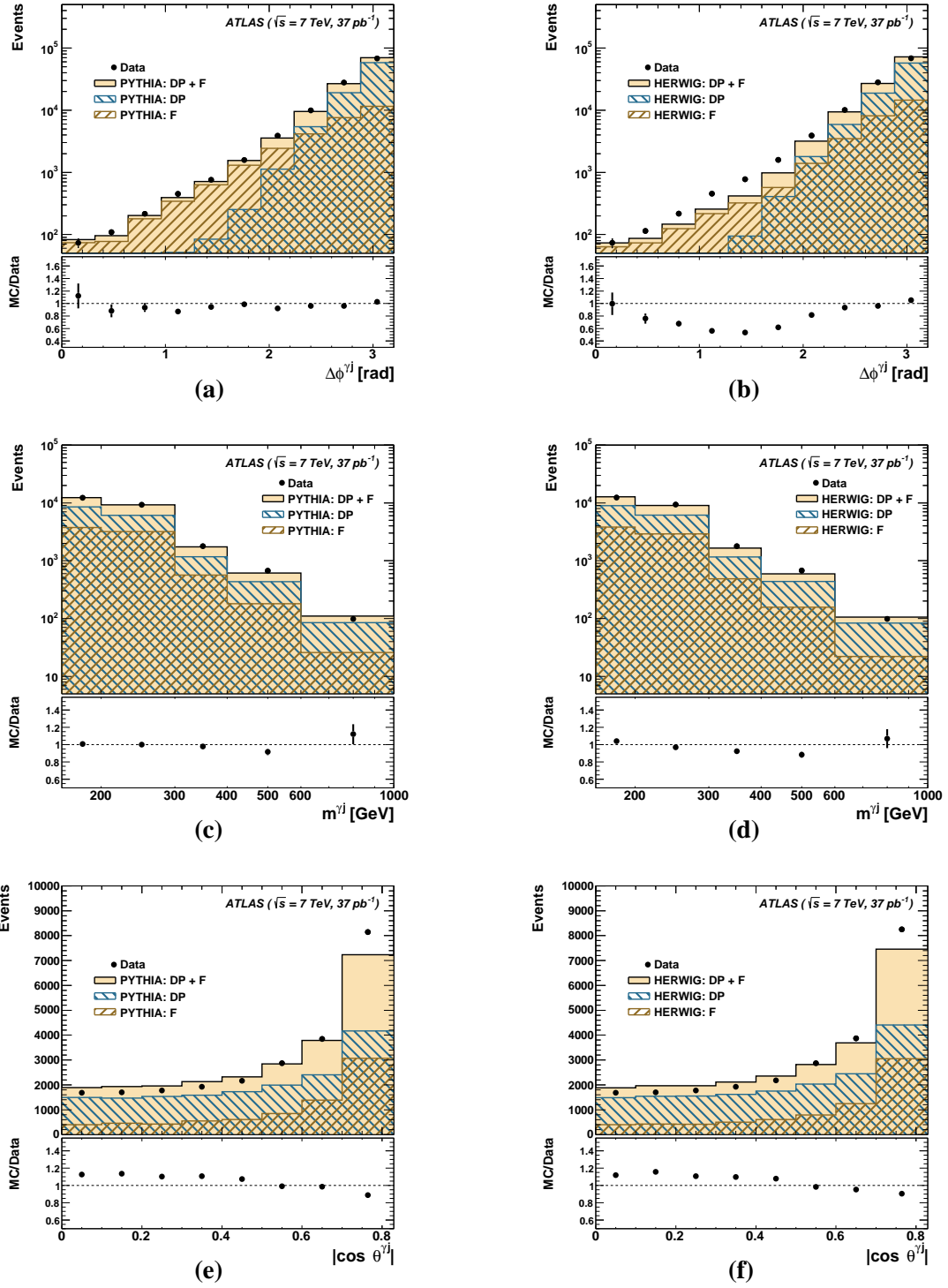
Figure 4: The estimated signal yield in data (dots) using the signal leakage fractions from (a,c,e) PYTHIA or (b,d,f) HERWIG as functions of (a,b) $\Delta\phi^{\gamma j}$, (c,d) $m^{\gamma j}$ and (e,f) $|\cos\theta^{\gamma j}|$. The distributions as functions of $m^{\gamma j}$ ($|\cos\theta^{\gamma j}|$) include requirements on $|\cos\theta^{\gamma j}|$ ($m^{\gamma j}$) and $|\eta^{\gamma} + y^{\text{jet}}|$ (see text). Other details as in the caption to Fig. 3.
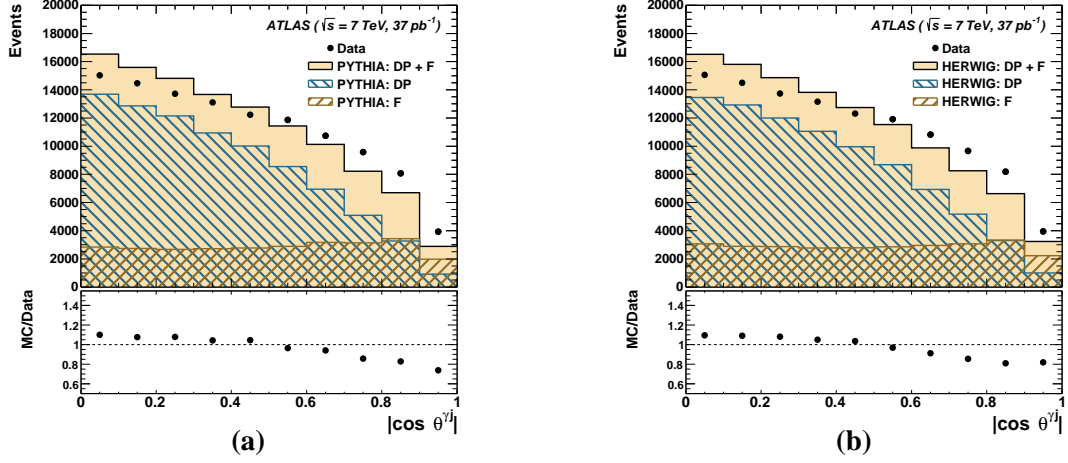
Figure 5: The estimated signal yield in data (dots) using the signal leakage fractions from (a) PYTHIA or (b) HERWIG as functions of $|\cos\theta^{\gamma j}|$. These distributions do not include requirements on $m^{\gamma j}$ or $|\eta^\gamma + y^{jet}|$. Other details as in the caption to Fig. 3.

and N_i^{part} is the number of MC events that pass the selection requirements at the particle level and are located in bin i. The bin-to-bin efficiencies are typically above 60%, except for p_T^{jet} and $\Delta\phi^{\gamma j}$ ($\gtrsim 40\%$) due to the limited resolution in these steeply falling distributions, and are similar for PYTHIA and HERWIG.

The bin-to-bin reconstruction purity was computed as $\kappa_i = N_i^{det,part}/N_i^{det}$, where N_i^{det} is the number of MC events that pass the selection requirements at the detector level and are located in bin i. The bin-to-bin reconstruction purities are typically above 70%, except for p_T^{jet} and $\Delta\phi^{\gamma j}$ ($\gtrsim 45\%$) due to the limited resolution in these steeply falling distributions, and are similar for PYTHIA and HERWIG.

The efficiency of the jet-quality criteria (see Section 3.2) applied to the data was estimated using a tag-and-probe method. The leading photon in each event was considered as the tag to probe the leading jet. Additional selection criteria, such as $\Delta\phi^{\gamma j} > 2.6$ (probe and tag required to be back-to-back) and $|p_T^{jet} - E_T^\gamma|/p_T^{avg} < 0.4$, where $p_T^{avg} = (p_T^{jet} + E_T^\gamma)/2$ (to have well-balanced probe and tag), were applied. The jet-quality criteria were then applied to the leading jet and the fraction of jets accepted was measured as a function of p_T^{jet} and $|y^{jet}|$. The jet-quality selection efficiency is approximately 99%. No correction for this efficiency was applied, but an uncertainty was included in the measurements (see Section 7).

6. Cross-section measurement procedure

Isolated-photon plus jet cross sections were measured for photons with $E_T^\gamma > 45$ GeV, $|\eta^\gamma| < 2.37$ (excluding the region $1.37 < |\eta^\gamma| < 1.52$) and $E_{T,part}^{iso} < 4$ GeV. The jets were reconstructed

13

Figure 6: The estimated signal yield in data (dots) using the signal leakage fractions from (a,c,e) PYTHIA or (b,d,f) HERWIG as functions of (a,b) E_T^γ, (c,d) p_T^{jet} and (e,f) $|y^{jet}|$. The direct-photon and fragmentation components of the MC simulations have been mixed using the value of α shown in each figure (see text). Other details as in the caption to Fig. 3.

14

Figure 7: The estimated signal yield in data (dots) using the signal leakage fractions from (a,c,e) PYTHIA or (b,d,f) HERWIG as functions of (a,b) $\Delta\phi^{\gamma j}$, (c,d) $m^{\gamma j}$ and (e,f) $|\cos\theta^{\gamma j}|$. The distributions as functions of $m^{\gamma j}$ ($|\cos\theta^{\gamma j}|$) include requirements on $|\cos\theta^{\gamma j}|$ ($m^{\gamma j}$) and $|\eta^\gamma + y^{\text{jet}}|$ (see text). Other details as in the caption to Fig. 6.

Figure 8: The estimated signal yield in data (dots) using the signal leakage fractions from (a) PYTHIA or (b) HERWIG as functions of $|\cos\theta^{\gamma j}|$. These distributions do not include requirements on $m^{\gamma j}$ or $|\eta^\gamma + y^{\rm jet}|$. Other details as in the caption to Fig. 6.

using the anti-k_t jet algorithm with $R = 0.6$ and selected with $p_{\rm T}^{\rm jet} > 40$ GeV, $|y^{\rm jet}| < 2.37$ and $\Delta R_{\gamma j} > 1$. Bin-averaged cross sections were measured as functions of $E_{\rm T}^\gamma$, $p_{\rm T}^{\rm jet}$, $|y^{\rm jet}|$ and $\Delta\phi^{\gamma j}$. Bin-averaged cross sections as functions of $m^{\gamma j}$ and $|\cos\theta^{\gamma j}|$ were measured in the kinematic region $|\eta^\gamma + y^{\rm jet}| < 2.37$, $|\cos\theta^{\gamma j}| < 0.83$ and $m^{\gamma j} > 161$ GeV. In addition, the bin-averaged cross section as a function of $|\cos\theta^{\gamma j}|$ was measured without the requirements on $m^{\gamma j}$ or $|\eta^\gamma + y^{\rm jet}|$.

The data distributions, after background subtraction, were corrected to the particle level using a bin-by-bin correction procedure. The bin-by-bin correction factors were determined using the MC samples; these correction factors took into account the efficiency of the selection criteria, jet and photon reconstruction as well as migration effects.

For this approach to be valid, the uncorrected distributions of the data must be adequately described by the MC simulations at the detector level. This condition was satisfied by both the PYTHIA and HERWIG MC samples after adjusting the relative fractions of the LO direct-photon and fragmentation components (see Section 5.1). The data distributions were corrected to the particle level via the formula

$$\frac{d\sigma}{dO}(i) = \frac{N_A^{\rm sig}(i)\, C^{\rm MC}(i)}{\mathcal{L}\, \Delta O(i)},$$

where $d\sigma/dO$ is the bin-averaged cross section as a function of observable $O = E_{\rm T}^\gamma$, $p_{\rm T}^{\rm jet}$, $|y^{\rm jet}|$, $\Delta\phi^{\gamma j}$, $m^{\gamma j}$ or $|\cos\theta^{\gamma j}|$, $N_A^{\rm sig}(i)$ is the number of background-subtracted data events in bin i, $C^{\rm MC}(i)$ is the correction factor in bin i, $\mathcal{L}$ is the integrated luminosity and $\Delta O(i)$ is the width of bin i. The bin-by-bin correction factors were computed as

$$C^{\text{MC}}(i) = \frac{\alpha\, N_{\text{part}}^{\text{MC,DP}}(i) + (1-\alpha)\, N_{\text{part}}^{\text{MC,F}}(i)}{\alpha\, N_{\text{det}}^{\text{MC,DP}}(i) + (1-\alpha)\, N_{\text{det}}^{\text{MC,F}}(i)},$$

where α corresponds to the optimised value obtained from the fit to the data for each observable, as explained in Section 5.1. The final bin-averaged cross sections were obtained from the average of the cross sections when using C^{MC} with MC = Pythia or Herwig. The uncertainties from the parton-shower and hadronisation models used for the corrections were estimated as the deviations from this average when using either Pythia or Herwig to correct the data (see Section 7). The correction factors differ from unity by typically 20% and are similar for Pythia and Herwig.

7. Systematic uncertainties

The following sources of systematic uncertainty were considered; average values, expressed in percent and shown in parentheses, quantify their effects on the cross section as a function of $|\cos\theta^{\gamma j}|$ (with the requirements on $m^{\gamma j}$ and $|\eta^\gamma + y^{\text{jet}}|$ applied):

- Simulation of the detector geometry. The systematic uncertainties originating from the limited knowledge of the material in the detector were evaluated by repeating the full analysis using a different detector simulation with increased material in front of the calorimeter [15]. This affects in particular the photon-conversion rate and the development of electromagnetic showers (±5%).

- Photon simulation and model and fit dependence. The MC simulation of the signal was used to estimate (i) the signal leakage fractions and (ii) the bin-by-bin correction factors:

  - For step (i), both the Pythia and Herwig simulations were used with the admixture of the direct-photon and fragmentation components as given by each MC simulation to yield two sets of background-subtracted data distributions. The signal leakage fractions depend on the relative fraction of the two components. The uncertainty related to the simulation of the isolated-photon components in the signal leakage fractions was estimated (conservatively) by performing the background subtraction with only the direct-photon or the fragmentation component (±3%).

  - For step (ii), the effects of the parton-shower and hadronisation models in the bin-by-bin correction factors were estimated as deviations from the nominal cross sections by using either only Pythia or only Herwig to correct the data (±1%).

  - The bin-by-bin correction factors also depend on the relative fractions of the two components; the nominal admixture was taken from the fit to the background-subtracted data distributions. A systematic uncertainty due to the fit was estimated (conservatively) by using the default admixture of the components (±2%).

- Jet and photon energy scale and resolution uncertainties. These uncertainties were estimated by varying both the electromagnetic and the jet energy scales and resolutions within their uncertainties [15, 19] (photon energy resolution: ±0.2%; photon energy scale: ±1%; jet energy resolution: ±1%; jet energy scale: ±5%).

17

- Uncertainty on the background correlation in the two-dimensional sideband method. In the background subtraction, $R^{\mathrm{bg}} = 1$ was assumed (see Section 5.1); i.e. the photon isolation and identification variables are uncorrelated for the background. This assumption was verified using both the data and simulated background samples and was found to hold within a 10% uncertainty in the kinematic region of the measurements presented here. The cross sections were recomputed accounting for possible correlations in the background subtraction, and the differences from the nominal results were taken as systematic uncertainties (±0.6%).

- Definition of the background control regions in the two-dimensional sideband method. The estimation of the contamination in the signal region is affected by the choice of the background control regions. The uncertainty due to this choice was estimated by repeating the analysis with different identification criteria and by changing the isolation boundary from the nominal value of 5 GeV to 4 or 6 GeV (±2%).

- Data-driven correction to the photon efficiency. The shower shapes of simulated photons in the calorimeter were corrected to improve the agreement with the data. The uncertainty on the photon-identification efficiency due to the application of these corrections was estimated using different simulated photon samples and a different detector simulation with increased material in front of the calorimeter [15] (±2%).

- Uncertainty on the jet reconstruction efficiency. The MC simulation reproduces the jet reconstruction efficiencies in the data to better than 1% [34] (±1%).

- Jet-quality selection efficiency. The efficiency of the jet-quality criteria was determined to be 99% (+1%).

- Uncertainty on the trigger efficiency (±0.7%).

- Uncertainty arising from the photon-isolation requirement. This uncertainty was evaluated by increasing the value of $E_{\mathrm{T,det}}^{\mathrm{iso}}$ in the MC simulations by the difference (+500 MeV) between the averages of $E_{\mathrm{T,det}}^{\mathrm{iso}}$ for electrons in simulation and data control samples [6] (+4%).

- Uncertainty on the integrated luminosity. The measurement of the luminosity has a ±3.4% uncertainty [16] (±3.4%).

For $d\sigma/dE_{\mathrm{T}}^{\gamma}$, the dominant uncertainties arise from the detector material in the simulation, the isolation requirement, the model dependence in the signal leakage fractions and the photon energy scale, though in some bins the uncertainty from the luminosity measurement provides the largest contribution. The dominant uncertainties for the other bin-averaged cross sections come from the detector simulation, the model dependence in the signal leakage fractions, the isolation requirement and the jet energy scale. All these systematic uncertainties were added in quadrature together with the statistical uncertainty and are shown as error bars in the figures of the measured cross sections (see Section 9).

8. Next-to-leading-order QCD calculations

The NLO QCD calculations used in this analysis were computed using the program JET-PHOX [35]. This program includes a full NLO QCD calculation of both the direct-photon and fragmentation contributions to the cross section.

The number of flavours was set to five. The renormalisation (μ_R), factorisation (μ_F) and fragmentation (μ_f) scales were chosen to be $\mu_R = \mu_F = \mu_f = E_T^\gamma$. The calculations were performed using the CTEQ6.6 [36] parameterisations of the proton PDFs and the NLO photon BFG set II photon fragmentation function [37]. The strong coupling constant was calculated at two-loop order with $\alpha_s(m_Z) = 0.118$. Predictions based on the CT10 [38] and MSTW2008nlo [39] proton PDF sets were also computed.

The calculations were performed using a parton-level isolation cut, which required a total transverse energy below 4 GeV from the partons inside a cone of radius $\Delta R = 0.4$ around the photon direction. The anti-k_t algorithm was applied to the partons in the events generated by this program to define jets of partons. The NLO QCD predictions were obtained using the photon and these jets of partons in each event.

8.1. Hadronisation and underlying-event corrections to the NLO QCD calculations

Since the measurements refer to jets of hadrons with the contribution from the underlying event included, whereas the NLO QCD calculations refer to jets of partons, the predictions were corrected to the particle level using the MC models. The multiplicative correction factor, C_{NLO}, was defined as the ratio of the cross section for jets of hadrons to that for jets of partons and was estimated by using the MC programs described in Section 4; a simulation of the underlying event was only included for the sample of events at particle level. The correction factors from PYTHIA and HERWIG are similar and close to unity, except at high p_T^{jet}; for $p_T^{\mathrm{jet}} > 200\,\mathrm{GeV}$, the value of C_{NLO} is 0.87 (0.82) for PYTHIA (HERWIG). The means of the factors obtained from PYTHIA and HERWIG were applied to the NLO QCD calculations.

8.2. Theoretical uncertainties

The following sources of uncertainty in the theoretical predictions were considered; average values, expressed in percent and shown in parentheses, quantify their effects on the cross section as a function of $|\cos\theta^{\gamma j}|$ (with the requirements on $m^{\gamma j}$ and $|\eta^\gamma + y^{\mathrm{jet}}|$ applied):

- The uncertainty on the NLO QCD calculations due to terms beyond NLO was estimated by repeating the calculations using values of μ_R, μ_F and μ_f scaled by the factors 0.5 and 2. The three scales were either varied simultaneously, individually or by fixing one and varying the other two. In all cases, the condition $0.5 \leq \mu_A/\mu_B \leq 2$ was imposed, where $A, B = R, F, f$ and $A \neq B$. The final uncertainty was taken as the largest deviation from the nominal value among the 14 possible variations ($\pm14\%$) and is dominated by the μ_R variations.

- The uncertainty on the NLO QCD calculations due to those on the proton PDFs was estimated by repeating the calculations using the 44 additional sets from the CTEQ6.6 error analysis ($\pm3.5\%$).

19

- The uncertainty on the NLO QCD calculations due to that on the value of $\alpha_s(m_Z)$ was estimated by repeating the calculations using two additional sets of proton PDFs, for which different values of $\alpha_s(m_Z)$ were assumed in the fits, namely $\alpha_s(m_Z) = 0.116$ and 0.120, following the prescription of Ref. [40] ($\pm 2.5\%$).

- The uncertainty on the NLO QCD calculations due to the modelling of the parton shower, hadronisation and underlying event was estimated by taking the difference of the C_{NLO} factors based on PYTHIA and HERWIG from their average ($\pm 0.5\%$).

For all observables, the dominant theoretical uncertainty is that arising from the terms beyond NLO. The total theoretical uncertainty was obtained by adding in quadrature the individual uncertainties listed above.

9. Results

The measured bin-averaged cross sections are presented in Figs. 9–14 and Tables 1–6. The measured $d\sigma/dE_T^\gamma$ and $d\sigma/dp_T^{\text{jet}}$ fall by three orders of magnitude in the measured range. The measured $d\sigma/d|y^{\text{jet}}|$ and $d\sigma/d\Delta\phi^{\gamma j}$ display a maximum at $|y^{\text{jet}}| \approx 0$ and $\Delta\phi^{\gamma j} \approx \pi$, respectively. The measured $d\sigma/dm^{\gamma j}$ ($d\sigma/d|\cos\theta^{\gamma j}|$) decreases (increases) as $m^{\gamma j}$ ($|\cos\theta^{\gamma j}|$) increases.

The predictions of the NLO QCD calculations from the JETPHOX program described in Section 8 and corrected for hadronisation and underlying-event effects are compared to the data in Figs. 9–14. The predictions give a good description of the E_T^γ and p_T^{jet} measured cross sections. The shape and normalisation of the measured cross section as a function of $|y^{\text{jet}}|$ is described well by the calculation in the whole range measured. For the maximum three-body final state of the NLO QCD calculations, the photon and the leading jet cannot be in the same hemisphere in the transverse plane, i.e. $\Delta\phi^{\gamma j}$ is necessarily larger than $\pi/2$; as a result, it is not unexpected that they fail to describe the measured $\Delta\phi^{\gamma j}$ distribution. The leading-logarithm parton-shower predictions of the PYTHIA, HERWIG and SHERPA MC models are also shown in Fig. 12; PYTHIA and SHERPA give a good description of the data in the whole range measured whereas HERWIG fails to do so. The measured cross sections as functions of $m^{\gamma j}$ and $|\cos\theta^{\gamma j}|$ are described well by the NLO QCD calculations.

The NLO QCD calculations based on the CT10 and MSTW2008nlo proton PDF sets are within the uncertainty band of the CTEQ6.6-based calculations. The shapes of the distributions from the three calculations are similar. The predictions based on the CTEQ6.6 and CT10 PDF sets are very similar in normalisation whereas those based on MSTW2008nlo are approximately 5% higher. All of these comparisons validate the description of the dynamics of isolated-photon plus jet production in pp collisions at $O(\alpha_{\text{em}}\alpha_s^2)$.

To gain further insight into the interpretation of the results, LO QCD predictions of the direct-photon and fragmentation contributions to the cross section were calculated. Even though at NLO the two components are no longer distinguishable, the LO calculations are useful to identify regions of phase space dominated by the fragmentation contribution and to illustrate the basic differences in the dynamics of the two processes. The ratio LO/NLO does (not) show a strong dependence on p_T^{jet} and $|\cos\theta^{\gamma j}|$ (E_T^γ, $|y^{\text{jet}}|$ and $m^{\gamma j}$). The LO and NLO QCD calculations as functions of $|\cos\theta^{\gamma j}|$ are compared in Fig. 15. The fragmentation contribution is observed to decrease

20
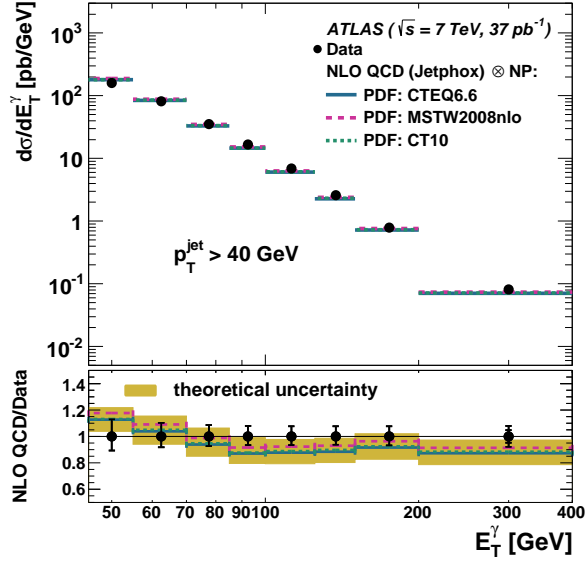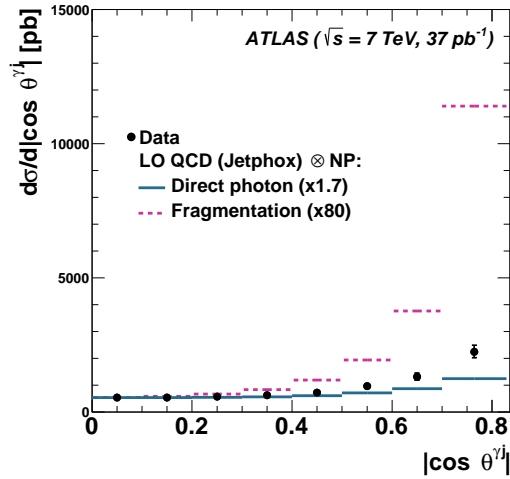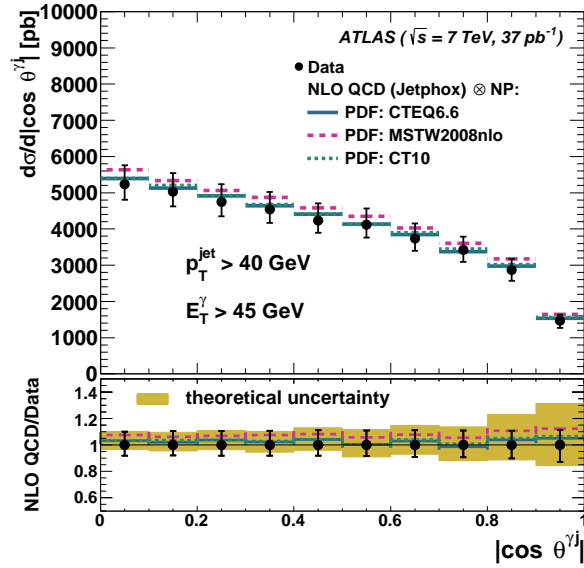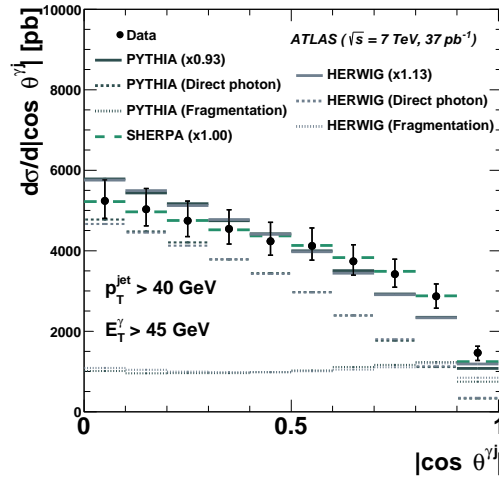
Figure 9: The measured bin-averaged cross section for isolated-photon plus jet production (dots) as a function of E_T^γ. The NLO QCD calculations from JETPHOX corrected for hadronisation and underlying-event effects (non-perturbative effects, NP) and using the CTEQ6.6 (solid lines), MSTW2008nlo (dashed lines) and CT10 (dotted lines) PDF sets are also shown. The bottom part of the figure shows the ratios of the NLO QCD calculations to the measured cross section. The inner (outer) error bars represent the statistical uncertainties (the statistical and systematic uncertainties added in quadrature) and the shaded band represents the theoretical uncertainty. For most of the points, the inner error bars are smaller than the marker size and, thus, not visible.
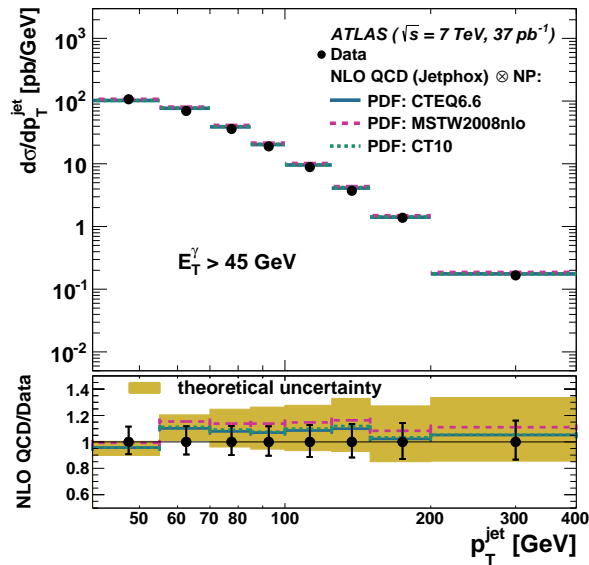
Figure 10: The measured bin-averaged cross section for isolated-photon plus jet production (dots) as a function of p_T^{jet}. Other details as in the caption to Fig. 9.
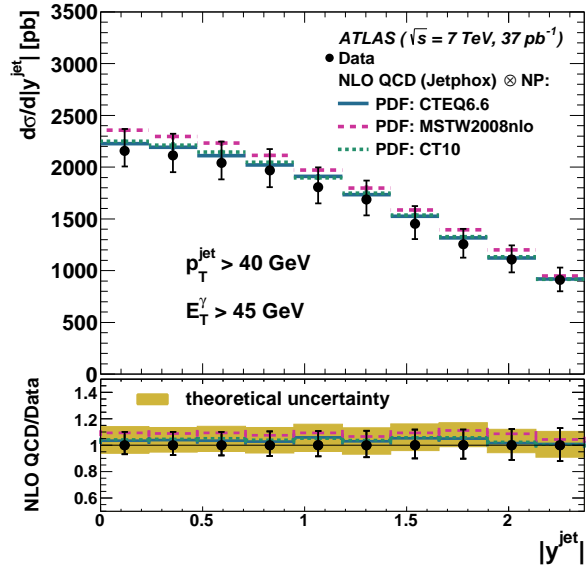
Figure 11: The measured bin-averaged cross section for isolated-photon plus jet production (dots) as a function of $|y^{jet}|$. Other details as in the caption to Fig. 9.
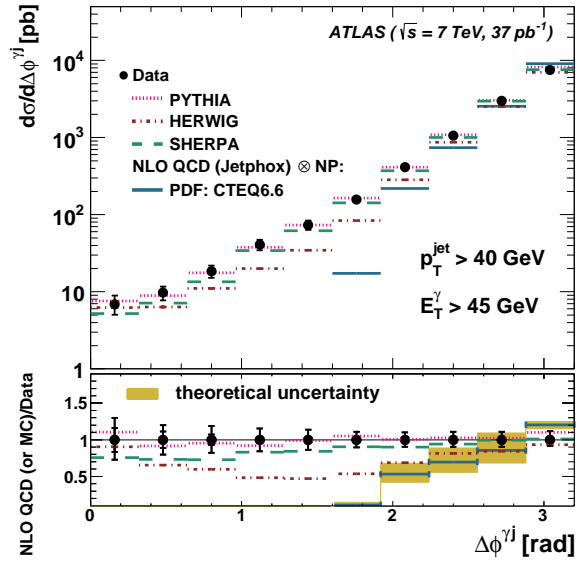
Figure 12: The measured bin-averaged cross section for isolated-photon plus jet production (dots) as a function of $\Delta\phi^{\gamma j}$. The predictions from the leading-logarithm parton-shower models of PYTHIA (dotted lines), HERWIG (dot-dashed lines) and SHERPA (long dashed lines) are also shown. Other details as in the caption to Fig. 9.
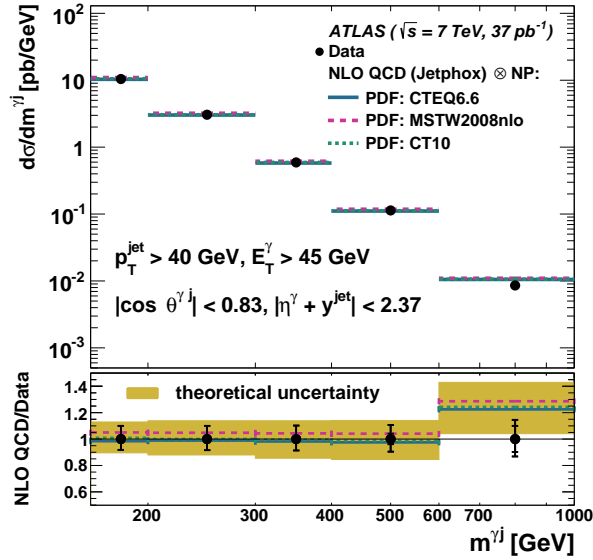
Figure 13: The measured bin-averaged cross section for isolated-photon plus jet production (dots) as a function of $m^{\gamma j}$ including the requirements on $|\cos\theta^{\gamma j}|$ and $|\eta^\gamma + y^{\text{jet}}|$. Other details as in the caption to Fig. 9.
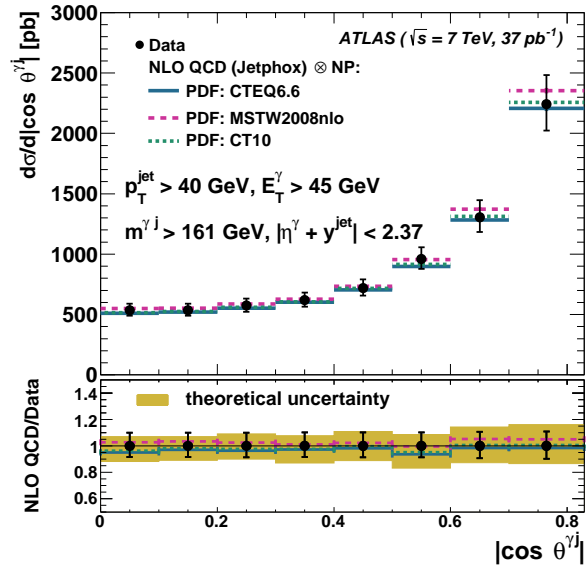
Figure 14: The measured bin-averaged cross section for isolated-photon plus jet production (dots) as a function of $|\cos\theta^{\gamma j}|$ including the requirements on $m^{\gamma j}$ and $|\eta^\gamma + y^{\text{jet}}|$. Other details as in the caption to Fig. 9.

as a function of E_T^γ, p_T^{jet} and $m^{\gamma j}$ and is approximately constant as a function of $|y^{jet}|$. However, it increases as a function of $|\cos\theta^{\gamma j}|$ from 2% up to 16%. Therefore, the regions at low E_T^γ, p_T^{jet} and $m^{\gamma j}$ as well as large $|\cos\theta^{\gamma j}|$ are expected to be sensitive to the fragmentation contribution.

The shapes of the bin-averaged cross sections for the direct-photon and fragmentation contributions at LO QCD were compared. The major difference is seen in the bin-averaged cross section as a function of $|\cos\theta^{\gamma j}|$ (see Fig. 16), with the contribution from fragmentation showing a steeper increase as $|\cos\theta^{\gamma j}| \to 1$ than that of direct-photon processes. This different behaviour is due to the different spin of the exchanged particle dominating each of the processes: a quark in the case of direct processes and a gluon in the case of fragmentation processes. Therefore, the distribution in $|\cos\theta^{\gamma j}|$ is particularly useful to study the dynamics underlying the hard process and the relative contributions of direct processes and fragmentation. The fact that the shape of the measured cross section $d\sigma/d|\cos\theta^{\gamma j}|$ is much closer to that of the direct-photon processes than that of fragmentation is consistent with the dominance of processes in which the exchanged particle is a quark. Furthermore, the increase of the cross section as $|\cos\theta^{\gamma j}| \to 1$ observed in the data is milder than that measured in dijet production in pp collisions [41], which is dominated by gluon exchange.

The measurement of the bin-averaged cross section as a function of $|\cos\theta^{\gamma j}|$ without the requirements on $m^{\gamma j}$ and $|\eta^\gamma + y^{jet}|$ is presented in Fig. 17 and Table 7. The decrease of the bin-averaged cross section as $|\cos\theta^{\gamma j}|$ increases is due to the non-uniform coverage in $|\cos\theta^{\gamma j}|$ induced by the requirements on the photon and jet rapidities and transverse momenta. The NLO QCD calculations are compared to the data in the same figure; they give a good description of the measured bin-averaged cross section. The comparison of the data to the predictions of Pythia, Herwig and Sherpa is shown in Fig. 18; in this figure, the MC calculations are normalised to the integrated measured cross section. The shapes of the predictions from Pythia and Herwig are very similar and do not describe the measured cross section. In these predictions, the contributions of direct-photon and fragmentation processes were added according to the MC default cross sections. It is possible to improve the description of the measured cross section by adjusting the relative contribution of the subprocesses, as demonstrated in Fig. 8 for the estimated signal yield. In contrast, the prediction of Sherpa gives a good description of the measured cross section, both in shape and magnitude; this may be attributable to the inclusion of higher-order contributions at tree-level in the prediction. The studies summarised in Figs. 17 and 18 give insight into the characteristics of one of the primary backgrounds in the study of the new particle discovered by ATLAS [12] and CMS [13] in the search for the Higgs boson.

10. Summary and conclusions

Bin-averaged cross sections for isolated photons in association with a jet in 7 TeV proton–proton collisions, $pp \to \gamma + jet + X$, have been presented using an integrated luminosity of 37.1 pb^{-1}. The jets were reconstructed using the anti-k_t jet algorithm with $R = 0.6$. Isolated-photon plus jet bin-averaged cross sections were measured as functions of E_T^γ, p_T^{jet}, $|y^{jet}|$, $\Delta\phi^{\gamma j}$, $m^{\gamma j}$ and $\cos\theta^{\gamma j}$. The bin-averaged cross sections $d\sigma/dm^{\gamma j}$ and $d\sigma/d|\cos\theta^{\gamma j}|$ were measured with additional selection criteria on $|\eta^\gamma + y^{jet}|$, $|\cos\theta^{\gamma j}|$ and $m^{\gamma j}$.

Regions of phase space sensitive to the contributions from fragmentation have been identified.
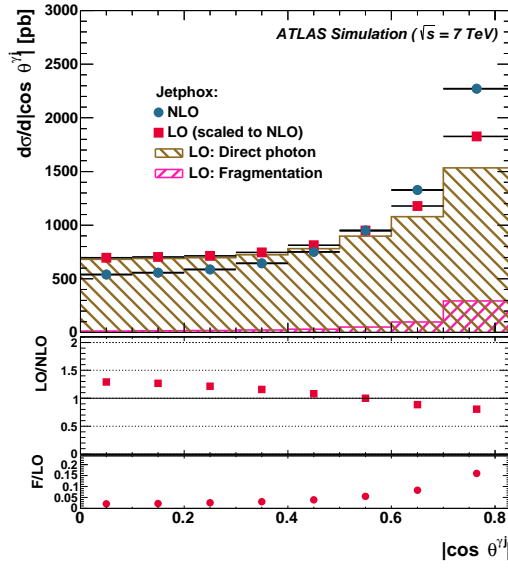
Figure 15: The NLO QCD predicted bin-averaged cross section for isolated-photon plus jet production as a function of $|\cos\theta^{\gamma j}|$ including the requirements on $m^{\gamma j}$ and $|\eta^\gamma + y^{jet}|$ (dots). The LO QCD calculation (squares) scaled to the NLO integrated cross section and the contributions of the direct-photon (right-hatched histogram) and fragmentation (left-hatched histogram) components are also shown. The middle part of the figure shows the ratio of the scaled LO to the NLO QCD calculations (squares); the bottom part of the figure shows the ratio of the fragmentation component to the full LO calculation (dots).

Figure 16: The measured bin-averaged cross section for isolated-photon plus jet production (dots) as a function of $|\cos\theta^{\gamma j}|$ including the requirements on $m^{\gamma j}$ and $|\eta^\gamma + y^{jet}|$. The direct-photon (solid lines) and fragmentation (dashed lines) components of the LO QCD prediction are also included. The calculations were normalised to the measured cross section for $|\cos\theta^{\gamma j}| < 0.1$; the factors used are shown in parentheses.

25

Figure 17: The measured bin-averaged cross section for isolated-photon plus jet production (dots) as a function of $|\cos\theta^{\gamma j}|$ without the requirements on $m^{\gamma j}$ and $|\eta^{\gamma} + y^{jet}|$. Other details as in the caption to Fig. 9.

Figure 18: The measured bin-averaged cross section for isolated-photon plus jet production (dots) as a function of $|\cos\theta^{\gamma j}|$ without the requirements on $m^{\gamma j}$ and $|\eta^{\gamma} + y^{jet}|$. The PYTHIA (dark lines) and HERWIG (light lines) MC calculations for the direct-photon (dashed lines), fragmentation (dotted lines) components and their sum (solid lines) are also shown. The prediction from SHERPA (long dashed lines) is also included. The full MC calculations are normalised to the integrated measured cross section. Other details as in the caption to Fig. 9.

As a result, these measurements can be used to tune the relative contributions of direct and fragmentation processes in the description of isolated-photon production by the Monte Carlo models.

The NLO QCD calculations, based on various proton PDFs and corrected for hadronisation and underlying-event effects using PYTHIA and HERWIG, have been compared to the measurements. The calculations give a reasonably good description of the measured cross sections both in shape and normalisation, except for $\Delta\phi^{\gamma j}$; this distribution is adequately described by the leading-order plus parton-shower prediction of PYTHIA or SHERPA. The measured dependence on $|\cos\theta^{\gamma j}|$ is consistent with the dominance of processes in which a quark is being exchanged.

A measurement of the bin-averaged cross section as a function of $|\cos\theta^{\gamma j}|$ without the requirements on $m^{\gamma j}$ and $|\eta^{\gamma}+y^{jet}|$ was also presented to understand the photon plus jet background relevant for the studies of the spin of the new particle observed by ATLAS and CMS in the search for the Higgs boson. The NLO QCD calculations give a good description of the data.

11. Acknowledgements

Table 1: The measured bin-averaged cross-section $d\sigma/dE_T^\gamma$ for isolated-photon plus jet production. The statistical (δ_{stat}) and systematic (δ_{syst}) uncertainties are shown separately. The corrections for hadronisation and underlying-event effects to be applied to the parton-level NLO QCD calculations (C_{NLO}) are shown in the last column. All tables with information on the measured cross sections, their uncertainties and correlations are available in HepData.

E_T^γ [GeV]	$d\sigma/dE_T^\gamma$ [pb/GeV]	δ_{stat} [pb/GeV]	δ_{syst} [pb/GeV]	C_{NLO}
$45 - 55$	160.2	± 0.9	$^{+20.6}_{-17.1}$	0.97
$55 - 70$	81.1	± 0.5	$^{+8.1}_{-6.7}$	0.95
$70 - 85$	35.39	± 0.32	$^{+3.00}_{-2.62}$	0.94
$85 - 100$	16.75	± 0.21	$^{+1.30}_{-1.11}$	0.92
$100 - 125$	6.89	± 0.10	$^{+0.52}_{-0.45}$	0.92
$125 - 150$	2.58	± 0.06	$^{+0.19}_{-0.16}$	0.92
$150 - 200$	0.789	± 0.025	$^{+0.054}_{-0.048}$	0.90
$200 - 400$	0.081	± 0.004	$^{+0.005}_{-0.005}$	0.91

Table 2: The measured bin-averaged cross-section $d\sigma/dp_T^{\text{jet}}$ for isolated-photon plus jet production. Other details as in the caption to Table 1.

p_T^{jet} [GeV]	$d\sigma/dp_T^{\text{jet}}$ [pb/GeV]	δ_{stat} [pb/GeV]	δ_{syst} [pb/GeV]	C_{NLO}
$40 - 55$	107.6	± 0.6	$^{+12.3}_{-10.0}$	0.96
$55 - 70$	70.1	± 0.5	$^{+8.2}_{-6.7}$	0.98
$70 - 85$	36.08	± 0.31	$^{+4.34}_{-3.61}$	0.96
$85 - 100$	18.99	± 0.22	$^{+2.21}_{-1.98}$	0.94
$100 - 125$	8.86	± 0.11	$^{+1.11}_{-1.00}$	0.91
$125 - 150$	3.74	± 0.07	$^{+0.50}_{-0.44}$	0.89
$150 - 200$	1.379	± 0.031	$^{+0.194}_{-0.179}$	0.86
$200 - 400$	0.167	± 0.005	$^{+0.026}_{-0.022}$	0.85

Table 3: The measured bin-averaged cross-section $d\sigma/d|y^{\text{jet}}|$ for isolated-photon plus jet production. Other details as in the caption to Table 1.

$|y^{\text{jet}}|$	$d\sigma/d|y^{\text{jet}}|$ [pb]	δ_{stat} [pb]	δ_{syst} [pb]	C_{NLO}
$0.000 - 0.237$	2158	± 20	$+211 \atop -148$	0.96
$0.237 - 0.474$	2113	± 20	$+208 \atop -161$	0.96
$0.474 - 0.711$	2043	± 20	$+203 \atop -159$	0.96
$0.711 - 0.948$	1968	± 20	$+204 \atop -160$	0.96
$0.948 - 1.185$	1806	± 19	$+191 \atop -153$	0.96
$1.185 - 1.422$	1687	± 18	$+183 \atop -153$	0.96
$1.422 - 1.659$	1452	± 17	$+171 \atop -147$	0.96
$1.659 - 1.896$	1256	± 16	$+147 \atop -130$	0.96
$1.896 - 2.133$	1108	± 15	$+135 \atop -123$	0.96
$2.133 - 2.370$	912	± 14	$+117 \atop -111$	0.95

Table 4: The measured bin-averaged cross-section $d\sigma/d\Delta\phi^{\gamma\text{j}}$ for isolated-photon plus jet production. Other details as in the caption to Table 1.

$\Delta\phi^{\gamma\text{j}}$ [rad]	$d\sigma/d\Delta\phi^{\gamma\text{j}}$ [pb]	δ_{stat} [pb]	δ_{syst} [pb]	C_{NLO}
$0.00 - 0.32$	6.9	± 1.1	$+1.7 \atop -1.5$	–
$0.32 - 0.64$	9.7	± 1.1	$+1.6 \atop -1.6$	–
$0.64 - 0.96$	18.5	± 1.3	$+3.2 \atop -3.0$	–
$0.96 - 1.28$	41.0	± 2.2	$+5.9 \atop -6.1$	–
$1.28 - 1.60$	73.6	± 2.9	$+9.7 \atop -9.5$	–
$1.60 - 1.92$	156	± 4	$+16 \atop -16$	0.91
$1.92 - 2.24$	412	± 8	$+41 \atop -38$	0.96
$2.24 - 2.56$	1063	± 12	$+113 \atop -101$	0.95
$2.56 - 2.88$	2985	± 21	$+328 \atop -281$	0.96
$2.88 - 3.20$	7518	± 34	$+868 \atop -623$	0.95

Table 5: The measured bin-averaged cross-section $d\sigma/dm^{\gamma j}$ with the requirements on $|\cos\theta^{\gamma j}|$ and $|\eta^\gamma + y^{\text{jet}}|$ for isolated-photon plus jet production. Other details as in the caption to Table 1.

$m^{\gamma j}$ [GeV]	$d\sigma/dm^{\gamma j}$ [pb/GeV]	δ_{stat} [pb/GeV]	δ_{syst} [pb/GeV]	C_{NLO}
$161 - 200$	10.46	± 0.11	$^{+1.03}_{-0.86}$	0.97
$200 - 300$	3.069	± 0.034	$^{+0.303}_{-0.255}$	0.95
$300 - 400$	0.594	± 0.015	$^{+0.058}_{-0.050}$	0.92
$400 - 600$	0.114	± 0.005	$^{+0.011}_{-0.010}$	0.91
$600 - 1000$	0.0086	± 0.0009	$^{+0.0009}_{-0.0008}$	0.91

Table 6: The measured bin-averaged cross-section $d\sigma/d|\cos\theta^{\gamma j}|$ with the requirements on $m^{\gamma j}$ and $|\eta^\gamma + y^{\text{jet}}|$ for isolated-photon plus jet production. Other details as in the caption to Table 1.

$|\cos\theta^{\gamma j}|$	$d\sigma/d|\cos\theta^{\gamma j}|$ [pb]	δ_{stat} [pb]	δ_{syst} [pb]	C_{NLO}
$0.00 - 0.10$	536	± 14	$^{+52}_{-43}$	0.94
$0.10 - 0.20$	536	± 14	$^{+52}_{-44}$	0.93
$0.20 - 0.30$	574	± 15	$^{+55}_{-48}$	0.94
$0.30 - 0.40$	619	± 15	$^{+61}_{-51}$	0.93
$0.40 - 0.50$	718	± 17	$^{+71}_{-60}$	0.94
$0.50 - 0.60$	960	± 19	$^{+94}_{-81}$	0.95
$0.60 - 0.70$	1306	± 23	$^{+137}_{-120}$	0.97
$0.70 - 0.83$	2242	± 29	$^{+239}_{-218}$	0.97

Table 7: The measured bin-averaged cross-section $d\sigma/d|\cos\theta^{\gamma j}|$ without the requirements on $m^{\gamma j}$ and $|\eta^{\gamma} + y^{\mathrm{jet}}|$ for isolated-photon plus jet production. Other details as in the caption to Table 1.

$\|\cos\theta^{\gamma j}\|$	$d\sigma/d\|\cos\theta^{\gamma j}\|$ [pb]	δ_{stat} [pb]	δ_{syst} [pb]	C_{NLO}
$0.0 - 0.1$	5240	± 50	$^{+520}_{-430}$	0.95
$0.1 - 0.2$	5030	± 50	$^{+520}_{-410}$	0.95
$0.2 - 0.3$	4750	± 50	$^{+490}_{-390}$	0.95
$0.3 - 0.4$	4540	± 50	$^{+480}_{-370}$	0.96
$0.4 - 0.5$	4240	± 40	$^{+470}_{-340}$	0.95
$0.5 - 0.6$	4120	± 40	$^{+450}_{-350}$	0.95
$0.6 - 0.7$	3740	± 40	$^{+410}_{-340}$	0.96
$0.7 - 0.8$	3420	± 40	$^{+370}_{-320}$	0.95
$0.8 - 0.9$	2870	± 40	$^{+300}_{-300}$	0.96
$0.9 - 1.0$	1460	± 30	$^{+160}_{-190}$	0.95

References

[1] D. d'Enterria and J. Rojo, Nucl. Phys. B 860 (2012) 311 [arXiv:1202.1762].

[2] L. Carminati et al., Europhys. Lett. 101 (2013) 61002 [arXiv:1212.5511].

[3] T. Pietrycki and A. Szczurek, Phys. Rev. D 76 (2007) 034003 [arXiv:0704.2158].

[4] Z. Belghobsi et al., Phys. Rev. D 79 (2009) 114024 [arXiv:0903.4834].

[5] ATLAS Collaboration, Phys. Rev. D 83 (2011) 052005 [arXiv:1012.4389].

[6] ATLAS Collaboration, Phys. Lett. B 706 (2011) 150 [arXiv:1108.0253].

[7] CMS Collaboration, Phys. Rev. Lett. 106 (2011) 082001 [arXiv:1012.0799].

[8] CMS Collaboration, Phys. Rev. D 84 (2011) 052011 [arXiv:1108.2044].

[9] ATLAS Collaboration, Phys. Rev. D 85 (2012) 092014 [arXiv:1203.3161].

[10] M. Cacciari, G.P. Salam and G. Soyez, JHEP 0804 (2008) 063 [arXiv:0802.1189].

[11] ATLAS Collaboration, Preprint arXiv:1307.1432 [hep-ex], 2013, submitted to Phys. Lett. B.

[12] ATLAS Collaboration, Phys. Lett. B 716 (2012) 1 [arXiv:1207.7214].

[13] CMS Collaboration, Phys. Lett. B 716 (2012) 30 [arXiv:1207.7235].

[14] ATLAS Collaboration, JINST 3 (2008) S08003.

[15] ATLAS Collaboration, Eur. Phys. J. C 72 (2012) 1909 [arXiv:1110.3174].

[16] ATLAS Collaboration, Preprint arXiv:1302.4393 [hep-ex], 2013, submitted to Eur. Phys. Jour. C.

[17] ATLAS Collaboration, ATLAS-PHYS-PUB-2011-007 (http://cds.cern.ch/record/1345329).

[18] ATLAS Collaboration, Preprint arXiv:0901.0512 [hep-ex], 2009.

[19] ATLAS Collaboration, Eur. Phys. J. C 73 (2013) 2304 [arXiv:1112.6426].

[20] T. Sjöstrand, S. Mrenna and P.Z. Skands, JHEP 0605 (2006) 026 [hep-ph/0603175].

[21] G. Corcella et al., JHEP 0101 (2001) 010 [hep-ph/0011363].

[22] B. Andersson et al., Phys. Rep. 97 (1983) 31.

[23] B.R. Webber, Nucl. Phys. B 238 (1984) 492.

[24] A. Sherstnev and R.S. Thorne, Eur. Phys. J. C 55 (2008) 553 [arXiv:0711.2473].

[25] A. Sherstnev and R.S. Thorne, Preprint arXiv:0807.2132 [hep-ph], 2008.

[26] J.M. Butterworth, J.R. Forshaw and M.H. Seymour, Z. Phys. C 72 (1996) 637 [hep-ph/9601371].

[27] ATLAS Collaboration, ATLAS-CONF-2010-031 (http://cds.cern.ch/record/1277665).

[28] ATLAS Collaboration, ATL-PHYS-PUB-2010-014 (http://cds.cern.ch/record/1303025).

[29] GEANT4 Collaboration, S. Agostinelli et al., Nucl. Inst. Meth. A 506 (2003) 250.

[30] ATLAS Collaboration, Eur. Phys. J. C 70 (2010) 823 [arXiv:1005.4568].

[31] T. Gleisberg et al., JHEP 0902 (2009) 007 [arXiv:0811.4622].

[32] J. Pumplin et al., JHEP 0207 (2002) 012 [hep-ph/0201195].

[33] C. Winter, F. Krauss and G. Soff, Eur. Phys. J. C 36 (2004) 381 [hep-ph/0311085].

[34] ATLAS Collaboration, Phys. Rev. D 86 (2012) 014022 [arXiv:1112.6297].

[35] S. Catani et al., JHEP 0205 (2002) 028 [hep-ph/0204023].

[36] P. Nadolsky et al., Phys. Rev. D 78 (2008) 013004 [arXiv:0802.0007].

[37] L. Bourhis, M. Fontannaz and J.Ph. Guillet, Eur. Phys. J. C 2 (1998) 529 [hep-ph/9704447].

[38] H.-L. Lai et al., Phys. Rev. D 82 (2010) 074024 [arXiv:1007.2241].

[39] A.D. Martin, W.J. Stirling, R.S. Thorne, G. Watt, Eur. Phys. J. C 64 (2009) 653 [arXiv:0905.3531].

[40] H.-L. Lai et al., Phys. Rev. D 82 (2010) 054021 [arXiv:1004.4624].

[41] ATLAS Collaboration, Eur. Phys. J. C 71 (2011) 1512 [arXiv:1009.5908].

The ATLAS Collaboration

G. Aad[48], T. Abajyan[21], B. Abbott[112], J. Abdallah[12], S. Abdel Khalek[116], A.A. Abdelalim[49],
O. Abdinov[11], R. Aben[106], B. Abi[113], M. Abolins[89], O.S. AbouZeid[159], H. Abramowicz[154],
H. Abreu[137], Y. Abulaiti[147a,147b], B.S. Acharya[165a,165b,a], L. Adamczyk[38a], D.L. Adams[25],
T.N. Addy[56], J. Adelman[177], S. Adomeit[99], T. Adye[130], S. Aefsky[23], T. Agatonovic-Jovin[13b],
J.A. Aguilar-Saavedra[125b,b], M. Agustoni[17], S.P. Ahlen[22], F. Ahles[48], A. Ahmad[149], M. Ahsan[41],
G. Aielli[134a,134b], T.P.A. Åkesson[80], G. Akimoto[156], A.V. Akimov[95], M.A. Alam[76], J. Albert[170],
S. Albrand[55], M.J. Alconada Verzini[70], M. Aleksa[30], I.N. Aleksandrov[64], F. Alessandria[90a],
C. Alexa[26a], G. Alexander[154], G. Alexandre[49], T. Alexopoulos[10], M. Alhroob[165a,165c], M. Aliev[16],
G. Alimonti[90a], J. Alison[31], B.M.M. Allbrooke[18], L.J. Allison[71], P.P. Allport[73],
S.E. Allwood-Spiers[53], J. Almond[83], A. Aloisio[103a,103b], R. Alon[173], A. Alonso[36], F. Alonso[70],
A. Altheimer[35], B. Alvarez Gonzalez[89], M.G. Alviggi[103a,103b], K. Amako[65],
Y. Amaral Coutinho[24a], C. Amelung[23], V.V. Ammosov[129,*], S.P. Amor Dos Santos[125a],
A. Amorim[125a,c], S. Amoroso[48], N. Amram[154], C. Anastopoulos[30], L.S. Ancu[17], N. Andari[30],
T. Andeen[35], C.F. Anders[58b], G. Anders[58a], K.J. Anderson[31], A. Andreazza[90a,90b], V. Andrei[58a],
X.S. Anduaga[70], S. Angelidakis[9], P. Anger[44], A. Angerami[35], F. Anghinolfi[30], A.V. Anisenkov[108],
N. Anjos[125a], A. Annovi[47], A. Antonaki[9], M. Antonelli[47], A. Antonov[97], J. Antos[145b],
F. Anulli[133a], M. Aoki[102], L. Aperio Bella[18], R. Apolle[119,d], G. Arabidze[89], I. Aracena[144],
Y. Arai[65], A.T.H. Arce[45], S. Arfaoui[149], J-F. Arguin[94], S. Argyropoulos[42], E. Arik[19a,*], M. Arik[19a],
A.J. Armbruster[88], O. Arnaez[82], V. Arnal[81], A. Artamonov[96], G. Artoni[133a,133b], D. Arutinov[21],
S. Asai[156], N. Asbah[94], S. Ask[28], B. Åsman[147a,147b], L. Asquith[6], K. Assamagan[25], R. Astalos[145a],
A. Astbury[170], M. Atkinson[166], B. Auerbach[6], E. Auge[116], K. Augsten[127], M. Aurousseau[146b],
G. Avolio[30], D. Axen[169], G. Azuelos[94,e], Y. Azuma[156], M.A. Baak[30], C. Bacci[135a,135b],
A.M. Bach[15], H. Bachacou[137], K. Bachas[155], M. Backes[49], M. Backhaus[21], J. Backus Mayes[144],
E. Badescu[26a], P. Bagiacchi[133a,133b], P. Bagnaia[133a,133b], Y. Bai[33a], D.C. Bailey[159], T. Bain[35],
J.T. Baines[130], O.K. Baker[177], S. Baker[77], P. Balek[128], F. Balli[137], E. Banas[39], P. Banerjee[94],
Sw. Banerjee[174], D. Banfi[30], A. Bangert[151], V. Bansal[170], H.S. Bansil[18], L. Barak[173],
S.P. Baranov[95], T. Barber[48], E.L. Barberio[87], D. Barberis[50a,50b], M. Barbero[84], D.Y. Bardin[64],
T. Barillari[100], M. Barisonzi[176], T. Barklow[144], N. Barlow[28], B.M. Barnett[130], R.M. Barnett[15],
A. Baroncelli[135a], G. Barone[49], A.J. Barr[119], F. Barreiro[81], J. Barreiro Guimarães da Costa[57],
R. Bartoldus[144], A.E. Barton[71], V. Bartsch[150], A. Basye[166], R.L. Bates[53], L. Batkova[145a],
J.R. Batley[28], A. Battaglia[17], M. Battistin[30], F. Bauer[137], H.S. Bawa[144,f], S. Beale[99], T. Beau[79],
P.H. Beauchemin[162], R. Beccherle[50a], P. Bechtle[21], H.P. Beck[17], K. Becker[176], S. Becker[99],
M. Beckingham[139], K.H. Becks[176], A.J. Beddall[19c], A. Beddall[19c], S. Bedikian[177],
V.A. Bednyakov[64], C.P. Bee[84], L.J. Beemster[106], T.A. Beermann[176], M. Begel[25],
C. Belanger-Champagne[86], P.J. Bell[49], W.H. Bell[49], G. Bella[154], L. Bellagamba[20a], A. Bellerive[29],
M. Bellomo[30], A. Belloni[57], O.L. Beloborodova[108,g], K. Belotskiy[97], O. Beltramello[30],
O. Benary[154], D. Benchekroun[136a], K. Bendtz[147a,147b], N. Benekos[166], Y. Benhammou[154],
E. Benhar Noccioli[49], J.A. Benitez Garcia[160b], D.P. Benjamin[45], J.R. Bensinger[23],
K. Benslama[131], S. Bentvelsen[106], D. Berge[30], E. Bergeaas Kuutmann[16], N. Berger[5],
F. Berghaus[170], E. Berglund[106], J. Beringer[15], P. Bernat[77], R. Bernhard[48], C. Bernius[78],
F.U. Bernlochner[170], T. Berry[76], C. Bertella[84], F. Bertolucci[123a,123b], M.I. Besana[90a,90b],

G.J. Besjes[105], N. Besson[137], S. Bethke[100], W. Bhimji[46], R.M. Bianchi[124], L. Bianchini[23],
M. Bianco[72a,72b], O. Biebel[99], S.P. Bieniek[77], K. Bierwagen[54], J. Biesiada[15], M. Biglietti[135a],
H. Bilokon[47], M. Bindi[20a,20b], S. Binet[116], A. Bingul[19c], C. Bini[133a,133b], B. Bittner[100],
C.W. Black[151], J.E. Black[144], K.M. Black[22], D. Blackburn[139], R.E. Blair[6], J.-B. Blanchard[137],
T. Blazek[145a], I. Bloch[42], C. Blocker[23], J. Blocki[39], W. Blum[82], U. Blumenschein[54],
G.J. Bobbink[106], V.S. Bobrovnikov[108], S.S. Bocchetta[80], A. Bocci[45], C.R. Boddy[119],
M. Boehler[48], J. Boek[176], T.T. Boek[176], N. Boelaert[36], J.A. Bogaerts[30], A.G. Bogdanchikov[108],
A. Bogouch[91,*], C. Bohm[147a], J. Bohm[126], V. Boisvert[76], T. Bold[38a], V. Boldea[26a], N.M. Bolnet[137],
M. Bomben[79], M. Bona[75], M. Boonekamp[137], S. Bordoni[79], C. Borer[17], A. Borisov[129],
G. Borissov[71], M. Borri[83], S. Borroni[42], J. Bortfeldt[99], V. Bortolotto[135a,135b], K. Bos[106],
D. Boscherini[20a], M. Bosman[12], H. Boterenbrood[106], J. Bouchami[94], J. Boudreau[124],
E.V. Bouhova-Thacker[71], D. Boumediene[34], C. Bourdarios[116], N. Bousson[84], S. Boutouil[136d],
A. Boveia[31], J. Boyd[30], I.R. Boyko[64], I. Bozovic-Jelisavcic[13b], J. Bracinik[18], P. Branchini[135a],
A. Brandt[8], G. Brandt[15], O. Brandt[54], U. Bratzler[157], B. Brau[85], J.E. Brau[115], H.M. Braun[176,*],
S.F. Brazzale[165a,165c], B. Brelier[159], J. Bremer[30], K. Brendlinger[121], R. Brenner[167], S. Bressler[173],
T.M. Bristow[46], D. Britton[53], F.M. Brochu[28], I. Brock[21], R. Brock[89], F. Broggi[90a], C. Bromberg[89],
J. Bronner[100], G. Brooijmans[35], T. Brooks[76], W.K. Brooks[32b], E. Brost[115], G. Brown[83],
P.A. Bruckman de Renstrom[39], D. Bruncko[145b], R. Bruneliere[48], S. Brunet[60], A. Bruni[20a],
G. Bruni[20a], M. Bruschi[20a], L. Bryngemark[80], T. Buanes[14], Q. Buat[55], F. Bucci[49], J. Buchanan[119],
P. Buchholz[142], R.M. Buckingham[119], A.G. Buckley[46], S.I. Buda[26a], I.A. Budagov[64],
B. Budick[109], L. Bugge[118], O. Bulekov[97], A.C. Bundock[73], M. Bunse[43], T. Buran[118,*],
H. Burckhart[30], S. Burdin[73], T. Burgess[14], S. Burke[130], E. Busato[34], V. Büscher[82], P. Bussey[53],
C.P. Buszello[167], B. Butler[57], J.M. Butler[22], C.M. Buttar[53], J.M. Butterworth[77], W. Buttinger[28],
M. Byszewski[10], S. Cabrera Urbán[168], D. Caforio[20a,20b], O. Cakir[4a], P. Calafiura[15], G. Calderini[79],
P. Calfayan[99], R. Calkins[107], L.P. Caloba[24a], R. Caloi[133a,133b], D. Calvet[34], S. Calvet[34],
R. Camacho Toro[49], P. Camarri[134a,134b], D. Cameron[118], L.M. Caminada[15],
R. Caminal Armadans[12], S. Campana[30], M. Campanelli[77], V. Canale[103a,103b], F. Canelli[31],
A. Canepa[160a], J. Cantero[81], R. Cantrill[76], T. Cao[40], M.D.M. Capeans Garrido[30], I. Caprini[26a],
M. Caprini[26a], D. Capriotti[100], M. Capua[37a,37b], R. Caputo[82], R. Cardarelli[134a], T. Carli[30],
G. Carlino[103a], L. Carminati[90a,90b], S. Caron[105], E. Carquin[32b], G.D. Carrillo-Montoya[146c],
A.A. Carter[75], J.R. Carter[28], J. Carvalho[125a,h], D. Casadei[109], M.P. Casado[12], M. Cascella[123a,123b],
C. Caso[50a,50b,*], E. Castaneda-Miranda[174], A. Castelli[106], V. Castillo Gimenez[168], N.F. Castro[125a],
G. Cataldi[72a], P. Catastini[57], A. Catinaccio[30], J.R. Catmore[30], A. Cattai[30], G. Cattani[134a,134b],
S. Caughron[89], V. Cavaliere[166], D. Cavalli[90a], M. Cavalli-Sforza[12], V. Cavasinni[123a,123b],
F. Ceradini[135a,135b], B. Cerio[45], A.S. Cerqueira[24b], A. Cerri[15], L. Cerrito[75], F. Cerutti[15],
A. Cervelli[17], S.A. Cetin[19b], A. Chafaq[136a], D. Chakraborty[107], I. Chalupkova[128], K. Chan[3],
P. Chang[166], B. Chapleau[86], J.D. Chapman[28], J.W. Chapman[88], D.G. Charlton[18], V. Chavda[83],
C.A. Chavez Barajas[30], S. Cheatham[86], S. Chekanov[6], S.V. Chekulaev[160a], G.A. Chelkov[64],
M.A. Chelstowska[105], C. Chen[63], H. Chen[25], S. Chen[33c], X. Chen[174], Y. Chen[35], Y. Cheng[31],
A. Cheplakov[64], R. Cherkaoui El Moursli[136e], V. Chernyatin[25], E. Cheu[7], S.L. Cheung[159],
L. Chevalier[137], V. Chiarella[47], G. Chiefari[103a,103b], J.T. Childers[30], A. Chilingarov[71],
G. Chiodini[72a], A.S. Chisholm[18], R.T. Chislett[77], A. Chitan[26a], M.V. Chizhov[64], G. Choudalakis[31],
S. Chouridou[9], B.K.B. Chow[99], I.A. Christidi[77], A. Christov[48], D. Chromek-Burckhart[30],

M.L. Chu[152], J. Chudoba[126], G. Ciapetti[133a,133b], A.K. Ciftci[4a], R. Ciftci[4a], D. Cinca[62], V. Cindro[74], A. Ciocio[15], M. Cirilli[88], P. Cirkovic[13b], Z.H. Citron[173], M. Citterio[90a], M. Ciubancan[26a], A. Clark[49], P.J. Clark[46], R.N. Clarke[15], J.C. Clemens[84], B. Clement[55], C. Clement[147a,147b], Y. Coadou[84], M. Cobal[165a,165c], A. Coccaro[139], J. Cochran[63], S. Coelli[90a], L. Coffey[23], J.G. Cogan[144], J. Coggeshall[166], J. Colas[5], S. Cole[107], A.P. Colijn[106], N.J. Collins[18], C. Collins-Tooth[53], J. Collot[55], T. Colombo[120a,120b], G. Colon[85], G. Compostella[100], P. Conde Muiño[125a], E. Coniavitis[167], M.C. Conidi[12], S.M. Consonni[90a,90b], V. Consorti[48], S. Constantinescu[26a], C. Conta[120a,120b], G. Conti[57], F. Conventi[103a,i], M. Cooke[15], B.D. Cooper[77], A.M. Cooper-Sarkar[119], N.J. Cooper-Smith[76], K. Copic[15], T. Cornelissen[176], M. Corradi[20a], F. Corriveau[86,j], A. Corso-Radu[164], A. Cortes-Gonzalez[166], G. Cortiana[100], G. Costa[90a], M.J. Costa[168], D. Costanzo[140], D. Côté[30], G. Cottin[32a], L. Courneyea[170], G. Cowan[76], B.E. Cox[83], K. Cranmer[109], S. Crépé-Renaudin[55], F. Crescioli[79], M. Cristinziani[21], G. Crosetti[37a,37b], C.-M. Cuciuc[26a], C. Cuenca Almenar[177], T. Cuhadar Donszelmann[140], J. Cummings[177], M. Curatolo[47], C.J. Curtis[18], C. Cuthbert[151], H. Czirr[142], P. Czodrowski[44], Z. Czyczula[177], S. D'Auria[53], M. D'Onofrio[73], A. D'Orazio[133a,133b], M.J. Da Cunha Sargedas De Sousa[125a], C. Da Via[83], W. Dabrowski[38a], A. Dafinca[119], T. Dai[88], F. Dallaire[94], C. Dallapiccola[85], M. Dam[36], D.S. Damiani[138], A.C. Daniells[18], H.O. Danielsson[30], V. Dao[105], G. Darbo[50a], G.L. Darlea[26c], S. Darmora[8], J.A. Dassoulas[42], W. Davey[21], T. Davidek[128], E. Davies[119,d], M. Davies[94], O. Davignon[79], A.R. Davison[77], Y. Davygora[58a], E. Dawe[143], I. Dawson[140], R.K. Daya-Ishmukhametova[23], K. De[8], R. de Asmundis[103a], S. De Castro[20a,20b], S. De Cecco[79], J. de Graat[99], N. De Groot[105], P. de Jong[106], C. De La Taille[116], H. De la Torre[81], F. De Lorenzi[63], L. De Nooij[106], D. De Pedis[133a], A. De Salvo[133a], U. De Sanctis[165a,165c], A. De Santo[150], J.B. De Vivie De Regie[116], G. De Zorzi[133a,133b], W.J. Dearnaley[71], R. Debbe[25], C. Debenedetti[46], B. Dechenaux[55], D.V. Dedovich[64], J. Degenhardt[121], J. Del Peso[81], T. Del Prete[123a,123b], T. Delemontex[55], M. Deliyergiyev[74], A. Dell'Acqua[30], L. Dell'Asta[22], M. Della Pietra[103a,i], D. della Volpe[103a,103b], M. Delmastro[5], P.A. Delsart[55], C. Deluca[106], S. Demers[177], M. Demichev[64], A. Demilly[79], B. Demirkoz[12,k], S.P. Denisov[129], D. Derendarz[39], J.E. Derkaoui[136d], F. Derue[79], P. Dervan[73], K. Desch[21], P.O. Deviveiros[106], A. Dewhurst[130], B. DeWilde[149], S. Dhaliwal[106], R. Dhullipudi[78,l], A. Di Ciaccio[134a,134b], L. Di Ciaccio[5], C. Di Donato[103a,103b], A. Di Girolamo[30], B. Di Girolamo[30], S. Di Luise[135a,135b], A. Di Mattia[153], B. Di Micco[135a,135b], R. Di Nardo[47], A. Di Simone[134a,134b], R. Di Sipio[20a,20b], M.A. Diaz[32a], E.B. Diehl[88], J. Dietrich[42], T.A. Dietzsch[58a], S. Diglio[87], K. Dindar Yagci[40], J. Dingfelder[21], F. Dinut[26a], C. Dionisi[133a,133b], P. Dita[26a], S. Dita[26a], F. Dittus[30], F. Djama[84], T. Djobava[51b], M.A.B. do Vale[24c], A. Do Valle Wemans[125a,m], T.K.O. Doan[5], D. Dobos[30], E. Dobson[77], J. Dodd[35], C. Doglioni[49], T. Doherty[53], T. Dohmae[156], Y. Doi[65,*], J. Dolejsi[128], Z. Dolezal[128], B.A. Dolgoshein[97,*], M. Donadelli[24d], J. Donini[34], J. Dopke[30], A. Doria[103a], A. Dos Anjos[174], A. Dotti[123a,123b], M.T. Dova[70], A.T. Doyle[53], M. Dris[10], J. Dubbert[88], S. Dube[15], E. Dubreuil[34], E. Duchovni[173], G. Duckeck[99], D. Duda[176], A. Dudarev[30], F. Dudziak[63], L. Duflot[116], M-A. Dufour[86], L. Duguid[76], M. Dührssen[30], M. Dunford[58a], H. Duran Yildiz[4a], M. Düren[52], M. Dwuznik[38a], J. Ebke[99], S. Eckweiler[82], W. Edson[2], C.A. Edwards[76], N.C. Edwards[53], W. Ehrenfeld[21], T. Eifert[144], G. Eigen[14], K. Einsweiler[15], E. Eisenhandler[75], T. Ekelof[167], M. El Kacimi[136c], M. Ellert[167], S. Elles[5], F. Ellinghaus[82], K. Ellis[75], N. Ellis[30], J. Elmsheuser[99], M. Elsing[30], D. Emeliyanov[130], Y. Enari[156], O.C. Endner[82], R. Engelmann[149], A. Engl[99],

J. Erdmann[177], A. Ereditato[17], D. Eriksson[147a], J. Ernst[2], M. Ernst[25], J. Ernwein[137], D. Errede[166],
S. Errede[166], E. Ertel[82], M. Escalier[116], H. Esch[43], C. Escobar[124], X. Espinal Curull[12],
B. Esposito[47], F. Etienne[84], A.I. Etienvre[137], E. Etzion[154], D. Evangelakou[54], H. Evans[60],
L. Fabbri[20a,20b], C. Fabre[30], G. Facini[30], R.M. Fakhrutdinov[129], S. Falciano[133a], Y. Fang[33a],
M. Fanti[90a,90b], A. Farbin[8], A. Farilla[135a], T. Farooque[159], S. Farrell[164], S.M. Farrington[171],
P. Farthouat[30], F. Fassi[168], P. Fassnacht[30], D. Fassouliotis[9], B. Fatholahzadeh[159], A. Favareto[90a,90b],
L. Fayard[116], P. Federic[145a], O.L. Fedin[122], W. Fedorko[169], M. Fehling-Kaschek[48], L. Feligioni[84],
C. Feng[33d], E.J. Feng[6], H. Feng[88], A.B. Fenyuk[129], J. Ferencei[145b], W. Fernando[6], S. Ferrag[53],
J. Ferrando[53], V. Ferrara[42], A. Ferrari[167], P. Ferrari[106], R. Ferrari[120a], D.E. Ferreira de Lima[53],
A. Ferrer[168], D. Ferrere[49], C. Ferretti[88], A. Ferretto Parodi[50a,50b], M. Fiascaris[31], F. Fiedler[82],
A. Filipčič[74], F. Filthaut[105], M. Fincke-Keeler[170], K.D. Finelli[45], M.C.N. Fiolhais[125a,h],
L. Fiorini[168], A. Firan[40], J. Fischer[176], M.J. Fisher[110], E.A. Fitzgerald[23], M. Flechl[48], I. Fleck[142],
P. Fleischmann[175], S. Fleischmann[176], G.T. Fletcher[140], G. Fletcher[75], T. Flick[176], A. Floderus[80],
L.R. Flores Castillo[174], A.C. Florez Bustos[160b], M.J. Flowerdew[100], T. Fonseca Martin[17],
A. Formica[137], A. Forti[83], D. Fortin[160a], D. Fournier[116], H. Fox[71], P. Francavilla[12],
M. Franchini[20a,20b], S. Franchino[30], D. Francis[30], M. Franklin[57], S. Franz[30], M. Fraternali[120a,120b],
S. Fratina[121], S.T. French[28], C. Friedrich[42], F. Friedrich[44], D. Froidevaux[30], J.A. Frost[28],
C. Fukunaga[157], E. Fullana Torregrosa[128], B.G. Fulsom[144], J. Fuster[168], C. Gabaldon[30],
O. Gabizon[173], A. Gabrielli[20a,20b], A. Gabrielli[133a,133b], S. Gadatsch[106], T. Gadfort[25],
S. Gadomski[49], G. Gagliardi[50a,50b], P. Gagnon[60], C. Galea[99], B. Galhardo[125a], E.J. Gallas[119],
V. Gallo[17], B.J. Gallop[130], P. Gallus[127], K.K. Gan[110], R.P. Gandrajula[62], Y.S. Gao[144,f],
A. Gaponenko[15], F.M. Garay Walls[46], F. Garberson[177], C. García[168], J.E. García Navarro[168],
M. Garcia-Sciveres[15], R.W. Gardner[31], N. Garelli[144], V. Garonne[30], C. Gatti[47], G. Gaudio[120a],
B. Gaur[142], L. Gauthier[94], P. Gauzzi[133a,133b], I.L. Gavrilenko[95], C. Gay[169], G. Gaycken[21],
E.N. Gazis[10], P. Ge[33d,n], Z. Gecse[169], C.N.P. Gee[130], D.A.A. Geerts[106], Ch. Geich-Gimbel[21],
K. Gellerstedt[147a,147b], C. Gemme[50a], A. Gemmell[53], M.H. Genest[55], S. Gentile[133a,133b],
M. George[54], S. George[76], D. Gerbaudo[164], A. Gershon[154], H. Ghazlane[136b], N. Ghodbane[34],
B. Giacobbe[20a], S. Giagu[133a,133b], V. Giangiobbe[12], P. Giannetti[123a,123b], F. Gianotti[30],
B. Gibbard[25], A. Gibson[159], S.M. Gibson[76], M. Gilchriese[15], T.P.S. Gillam[28], D. Gillberg[30],
A.R. Gillman[130], D.M. Gingrich[3,e], N. Giokaris[9], M.P. Giordani[165c], R. Giordano[103a,103b],
F.M. Giorgi[16], P. Giovannini[100], P.F. Giraud[137], D. Giugni[90a], C. Giuliani[48], M. Giunta[94],
B.K. Gjelsten[118], I. Gkialas[155,o], L.K. Gladilin[98], C. Glasman[81], J. Glatzer[21], A. Glazov[42],
G.L. Glonti[64], M. Goblirsch-kolb[100], J.R. Goddard[75], J. Godfrey[143], J. Godlewski[30], M. Goebel[42],
C. Goeringer[82], S. Goldfarb[88], T. Golling[177], D. Golubkov[129], A. Gomes[125a,c],
L.S. Gomez Fajardo[42], R. Gonçalo[76], J. Goncalves Pinto Firmino Da Costa[42], L. Gonella[21],
S. González de la Hoz[168], G. Gonzalez Parra[12], M.L. Gonzalez Silva[27], S. Gonzalez-Sevilla[49],
J.J. Goodson[149], L. Goossens[30], P.A. Gorbounov[96], H.A. Gordon[25], I. Gorelov[104], G. Gorfine[176],
B. Gorini[30], E. Gorini[72a,72b], A. Gorišek[74], E. Gornicki[39], A.T. Goshaw[6], C. Gössling[43],
M.I. Gostkin[64], I. Gough Eschrich[164], M. Gouighri[136a], D. Goujdami[136c], M.P. Goulette[49],
A.G. Goussiou[139], C. Goy[5], S. Gozpinar[23], L. Graber[54], I. Grabowska-Bold[38a], P. Grafström[20a,20b],
K-J. Grahn[42], E. Gramstad[118], F. Grancagnolo[72a], S. Grancagnolo[16], V. Grassi[149], V. Gratchev[122],
H.M. Gray[30], J.A. Gray[149], E. Graziani[135a], O.G. Grebenyuk[122], T. Greenshaw[73],
Z.D. Greenwood[78,l], K. Gregersen[36], I.M. Gregor[42], P. Grenier[144], J. Griffiths[8], N. Grigalashvili[64],

A.A. Grillo[138], K. Grimm[71], S. Grinstein[12,p], Ph. Gris[34], Y.V. Grishkevich[98], J.-F. Grivaz[116],
J.P. Grohs[44], A. Grohsjean[42], E. Gross[173], J. Grosse-Knetter[54], J. Groth-Jensen[173], K. Grybel[142],
F. Guescini[49], D. Guest[177], O. Gueta[154], C. Guicheney[34], E. Guido[50a,50b], T. Guillemin[116],
S. Guindon[2], U. Gul[53], J. Gunther[127], J. Guo[35], P. Gutierrez[112], N. Guttman[154], O. Gutzwiller[174],
C. Guyot[137], C. Gwenlan[119], C.B. Gwilliam[73], A. Haas[109], S. Haas[30], C. Haber[15],
H.K. Hadavand[8], P. Haefner[21], Z. Hajduk[39], H. Hakobyan[178], D. Hall[119], G. Halladjian[62],
K. Hamacher[176], P. Hamal[114], K. Hamano[87], M. Hamer[54], A. Hamilton[146a,q], S. Hamilton[162],
L. Han[33b], K. Hanagaki[117], K. Hanawa[161], M. Hance[15], C. Handel[82], P. Hanke[58a], J.R. Hansen[36],
J.B. Hansen[36], J.D. Hansen[36], P.H. Hansen[36], P. Hansson[144], K. Hara[161], A.S. Hard[174],
T. Harenberg[176], S. Harkusha[91], D. Harper[88], R.D. Harrington[46], O.M. Harris[139], J. Hartert[48],
F. Hartjes[106], T. Haruyama[65], A. Harvey[56], S. Hasegawa[102], Y. Hasegawa[141], S. Hassani[137],
S. Haug[17], M. Hauschild[30], R. Hauser[89], M. Havranek[21], C.M. Hawkes[18], R.J. Hawkings[30],
A.D. Hawkins[80], T. Hayakawa[66], T. Hayashi[161], D. Hayden[76], C.P. Hays[119], H.S. Hayward[73],
S.J. Haywood[130], S.J. Head[18], T. Heck[82], V. Hedberg[80], L. Heelan[8], S. Heim[121], B. Heinemann[15],
S. Heisterkamp[36], J. Hejbal[126], L. Helary[22], C. Heller[99], M. Heller[30], S. Hellman[147a,147b],
D. Hellmich[21], C. Helsens[30], J. Henderson[119], R.C.W. Henderson[71], M. Henke[58a], A. Henrichs[177],
A.M. Henriques Correia[30], S. Henrot-Versille[116], C. Hensel[54], G.H. Herbert[16], C.M. Hernandez[8],
Y. Hernández Jiménez[168], R. Herrberg-Schubert[16], G. Herten[48], R. Hertenberger[99], L. Hervas[30],
G.G. Hesketh[77], N.P. Hessey[106], R. Hickling[75], E. Higón-Rodriguez[168], J.C. Hill[28], K.H. Hiller[42],
S. Hillert[21], S.J. Hillier[18], I. Hinchliffe[15], E. Hines[121], M. Hirose[117], D. Hirschbuehl[176],
J. Hobbs[149], N. Hod[106], M.C. Hodgkinson[140], P. Hodgson[140], A. Hoecker[30], M.R. Hoeferkamp[104],
J. Hoffman[40], D. Hoffmann[84], J.I. Hofmann[58a], M. Hohlfeld[82], S.O. Holmgren[147a],
J.L. Holzbauer[89], T.M. Hong[121], L. Hooft van Huysduynen[109], J-Y. Hostachy[55], S. Hou[152],
A. Hoummada[136a], J. Howard[119], J. Howarth[83], M. Hrabovsky[114], I. Hristova[16], J. Hrivnac[116],
T. Hryn'ova[5], P.J. Hsu[82], S.-C. Hsu[139], D. Hu[35], X. Hu[25], Z. Hubacek[30], F. Hubaut[84],
F. Huegging[21], A. Huettmann[42], T.B. Huffman[119], E.W. Hughes[35], G. Hughes[71], M. Huhtinen[30],
T.A. Hülsing[82], M. Hurwitz[15], N. Huseynov[64,r], J. Huston[89], J. Huth[57], G. Iacobucci[49],
G. Iakovidis[10], I. Ibragimov[142], L. Iconomidou-Fayard[116], J. Idarraga[116], P. Iengo[103a],
O. Igonkina[106], Y. Ikegami[65], K. Ikematsu[142], M. Ikeno[65], D. Iliadis[155], N. Ilic[159], T. Ince[100],
P. Ioannou[9], M. Iodice[135a], K. Iordanidou[9], V. Ippolito[133a,133b], A. Irles Quiles[168], C. Isaksson[167],
M. Ishino[67], M. Ishitsuka[158], R. Ishmukhametov[110], C. Issever[119], S. Istin[19a], A.V. Ivashin[129],
W. Iwanski[39], H. Iwasaki[65], J.M. Izen[41], V. Izzo[103a], B. Jackson[121], J.N. Jackson[73], P. Jackson[1],
M.R. Jaekel[30], V. Jain[2], K. Jakobs[48], S. Jakobsen[36], T. Jakoubek[126], J. Jakubek[127], D.O. Jamin[152],
D.K. Jana[112], E. Jansen[77], H. Jansen[30], J. Janssen[21], A. Jantsch[100], M. Janus[48], R.C. Jared[174],
G. Jarlskog[80], L. Jeanty[57], G.-Y. Jeng[151], I. Jen-La Plante[31], D. Jennens[87], P. Jenni[30], J. Jentzsch[43],
C. Jeske[171], S. Jézéquel[5], M.K. Jha[20a], H. Ji[174], W. Ji[82], J. Jia[149], Y. Jiang[33b],
M. Jimenez Belenguer[42], S. Jin[33a], O. Jinnouchi[158], M.D. Joergensen[36], D. Joffe[40],
M. Johansen[147a,147b], K.E. Johansson[147a], P. Johansson[140], S. Johnert[42], K.A. Johns[7],
K. Jon-And[147a,147b], G. Jones[171], R.W.L. Jones[71], T.J. Jones[73], P.M. Jorge[125a], K.D. Joshi[83],
J. Jovicevic[148], X. Ju[174], C.A. Jung[43], R.M. Jungst[30], P. Jussel[61], A. Juste Rozas[12,p], S. Kabana[17],
M. Kaci[168], A. Kaczmarska[39], P. Kadlecik[36], M. Kado[116], H. Kagan[110], M. Kagan[144],
E. Kajomovitz[153], S. Kalinin[176], S. Kama[40], N. Kanaya[156], M. Kaneda[30], S. Kaneti[28], T. Kanno[158],
V.A. Kantserov[97], J. Kanzaki[65], B. Kaplan[109], A. Kapliy[31], D. Kar[53], K. Karakostas[10],

M. Karnevskiy[82], V. Kartvelishvili[71], A.N. Karyukhin[129], L. Kashif[174], G. Kasieczka[58b],
R.D. Kass[110], A. Kastanas[14], Y. Kataoka[156], J. Katzy[42], V. Kaushik[7], K. Kawagoe[69],
T. Kawamoto[156], G. Kawamura[54], S. Kazama[156], V.F. Kazanin[108], M.Y. Kazarinov[64], R. Keeler[170],
P.T. Keener[121], R. Kehoe[40], M. Keil[54], J.S. Keller[139], H. Keoshkerian[5], O. Kepka[126],
B.P. Kerševan[74], S. Kersten[176], K. Kessoku[156], J. Keung[159], F. Khalil-zada[11],
H. Khandanyan[147a,147b], A. Khanov[113], D. Kharchenko[64], A. Khodinov[97], A. Khomich[58a],
T.J. Khoo[28], G. Khoriauli[21], A. Khoroshilov[176], V. Khovanskiy[96], E. Khramov[64], J. Khubua[51b],
H. Kim[147a,147b], S.H. Kim[161], N. Kimura[172], O. Kind[16], B.T. King[73], M. King[66], R.S.B. King[119],
S.B. King[169], J. Kirk[130], A.E. Kiryunin[100], T. Kishimoto[66], D. Kisielewska[38a], T. Kitamura[66],
T. Kittelmann[124], K. Kiuchi[161], E. Kladiva[145b], M. Klein[73], U. Klein[73], K. Kleinknecht[82],
M. Klemetti[86], A. Klier[173], P. Klimek[147a,147b], A. Klimentov[25], R. Klingenberg[43], J.A. Klinger[83],
E.B. Klinkby[36], T. Klioutchnikova[30], P.F. Klok[105], E.-E. Kluge[58a], P. Kluit[106], S. Kluth[100],
E. Kneringer[61], E.B.F.G. Knoops[84], A. Knue[54], B.R. Ko[45], T. Kobayashi[156], M. Kobel[44],
M. Kocian[144], P. Kodys[128], S. Koenig[82], F. Koetsveld[105], P. Koevesarki[21], T. Koffas[29],
E. Koffeman[106], L.A. Kogan[119], S. Kohlmann[176], F. Kohn[54], Z. Kohout[127], T. Kohriki[65], T. Koi[144],
H. Kolanoski[16], I. Koletsou[90a], J. Koll[89], A.A. Komar[95], Y. Komori[156], T. Kondo[65], K. Köneke[30],
A.C. König[105], T. Kono[42,s], A.I. Kononov[48], R. Konoplich[109,t], N. Konstantinidis[77],
R. Kopeliansky[153], S. Koperny[38a], L. Köpke[82], A.K. Kopp[48], K. Korcyl[39], K. Kordas[155],
A. Korn[46], A.A. Korol[108], I. Korolkov[12], E.V. Korolkova[140], V.A. Korotkov[129], O. Kortner[100],
S. Kortner[100], V.V. Kostyukhin[21], S. Kotov[100], V.M. Kotov[64], A. Kotwal[45], C. Kourkoumelis[9],
V. Kouskoura[155], A. Koutsman[160a], R. Kowalewski[170], T.Z. Kowalski[38a], W. Kozanecki[137],
A.S. Kozhin[129], V. Kral[127], V.A. Kramarenko[98], G. Kramberger[74], M.W. Krasny[79],
A. Krasznahorkay[109], J.K. Kraus[21], A. Kravchenko[25], S. Kreiss[109], J. Kretzschmar[73],
K. Kreutzfeldt[52], N. Krieger[54], P. Krieger[159], K. Kroeninger[54], H. Kroha[100], J. Kroll[121],
J. Kroseberg[21], J. Krstic[13a], U. Kruchonak[64], H. Krüger[21], T. Kruker[17], N. Krumnack[63],
Z.V. Krumshteyn[64], A. Kruse[174], M.K. Kruse[45], M. Kruskal[22], T. Kubota[87], S. Kuday[4a],
S. Kuehn[48], A. Kugel[58c], T. Kuhl[42], V. Kukhtin[64], Y. Kulchitsky[91], S. Kuleshov[32b], M. Kuna[79],
J. Kunkle[121], A. Kupco[126], H. Kurashige[66], M. Kurata[161], Y.A. Kurochkin[91], V. Kus[126],
E.S. Kuwertz[148], M. Kuze[158], J. Kvita[143], R. Kwee[16], A. La Rosa[49], L. La Rotonda[37a,37b],
L. Labarga[81], S. Lablak[136a], C. Lacasta[168], F. Lacava[133a,133b], J. Lacey[29], H. Lacker[16], D. Lacour[79],
V.R. Lacuesta[168], E. Ladygin[64], R. Lafaye[5], B. Laforge[79], T. Lagouri[177], S. Lai[48], H. Laier[58a],
E. Laisne[55], L. Lambourne[77], C.L. Lampen[7], W. Lampl[7], E. Lançon[137], U. Landgraf[48],
M.P.J. Landon[75], V.S. Lang[58a], C. Lange[42], A.J. Lankford[164], F. Lanni[25], K. Lantzsch[30],
A. Lanza[120a], S. Laplace[79], C. Lapoire[21], J.F. Laporte[137], T. Lari[90a], A. Larner[119], M. Lassnig[30],
P. Laurelli[47], V. Lavorini[37a,37b], W. Lavrijsen[15], P. Laycock[73], O. Le Dortz[79], E. Le Guirriec[84],
E. Le Menedeu[12], T. LeCompte[6], F. Ledroit-Guillon[55], H. Lee[106], J.S.H. Lee[117], S.C. Lee[152],
L. Lee[177], G. Lefebvre[79], M. Lefebvre[170], M. Legendre[137], F. Legger[99], C. Leggett[15],
M. Lehmacher[21], G. Lehmann Miotto[30], A.G. Leister[177], M.A.L. Leite[24d], R. Leitner[128],
D. Lellouch[173], B. Lemmer[54], V. Lendermann[58a], K.J.C. Leney[146c], T. Lenz[106], G. Lenzen[176],
B. Lenzi[30], K. Leonhardt[44], S. Leontsinis[10], F. Lepold[58a], C. Leroy[94], J-R. Lessard[170],
C.G. Lester[28], C.M. Lester[121], J. Levêque[5], D. Levin[88], L.J. Levinson[173], A. Lewis[119],
G.H. Lewis[109], A.M. Leyko[21], M. Leyton[16], B. Li[33b,u], B. Li[84], H. Li[149], H.L. Li[31], S. Li[45], X. Li[88],
Z. Liang[119,v], H. Liao[34], B. Liberti[134a], P. Lichard[30], K. Lie[166], J. Liebal[21], W. Liebig[14],

C. Limbach[21], A. Limosani[87], M. Limper[62], S.C. Lin[152,w], F. Linde[106], B.E. Lindquist[149], J.T. Linnemann[89], E. Lipeles[121], A. Lipniacka[14], M. Lisovyi[42], T.M. Liss[166], D. Lissauer[25], A. Lister[169], A.M. Litke[138], D. Liu[152], J.B. Liu[33b], K. Liu[33b,x], L. Liu[88], M. Liu[45], M. Liu[33b], Y. Liu[33b], M. Livan[120a,120b], S.S.A. Livermore[119], A. Lleres[55], J. Llorente Merino[81], S.L. Lloyd[75], F. Lo Sterzo[133a,133b], E. Lobodzinska[42], P. Loch[7], W.S. Lockman[138], T. Loddenkoetter[21], F.K. Loebinger[83], A.E. Loevschall-Jensen[36], A. Loginov[177], C.W. Loh[169], T. Lohse[16], K. Lohwasser[48], M. Lokajicek[126], V.P. Lombardo[5], R.E. Long[71], L. Lopes[125a], D. Lopez Mateos[57], J. Lorenz[99], N. Lorenzo Martinez[116], M. Losada[163], P. Loscutoff[15], M.J. Losty[160a,*], X. Lou[41], A. Lounis[116], K.F. Loureiro[163], J. Love[6], P.A. Love[71], A.J. Lowe[144,f], F. Lu[33a], H.J. Lubatti[139], C. Luci[133a,133b], A. Lucotte[55], D. Ludwig[42], I. Ludwig[48], J. Ludwig[48], F. Luehring[60], W. Lukas[61], L. Luminari[133a], E. Lund[118], J. Lundberg[147a,147b], O. Lundberg[147a,147b], B. Lund-Jensen[148], J. Lundquist[36], M. Lungwitz[82], D. Lynn[25], R. Lysak[126], E. Lytken[80], H. Ma[25], L.L. Ma[174], G. Maccarrone[47], A. Macchiolo[100], B. Maček[74], J. Machado Miguens[125a], D. Macina[30], R. Mackeprang[36], R. Madar[48], R.J. Madaras[15], H.J. Maddocks[71], W.F. Mader[44], A. Madsen[167], M. Maeno[5], T. Maeno[25], L. Magnoni[164], E. Magradze[54], K. Mahboubi[48], J. Mahlstedt[106], S. Mahmoud[73], G. Mahout[18], C. Maiani[137], C. Maidantchik[24a], A. Maio[125a,c], S. Majewski[115], Y. Makida[65], N. Makovec[116], P. Mal[137,y], B. Malaescu[79], Pa. Malecki[39], P. Malecki[39], V.P. Maleev[122], F. Malek[55], U. Mallik[62], D. Malon[6], C. Malone[144], S. Maltezos[10], V.M. Malyshev[108], S. Malyukov[30], J. Mamuzic[13b], L. Mandelli[90a], I. Mandić[74], R. Mandrysch[62], J. Maneira[125a], A. Manfredini[100], L. Manhaes de Andrade Filho[24b], J.A. Manjarres Ramos[137], A. Mann[99], P.M. Manning[138], A. Manousakis-Katsikakis[9], B. Mansoulie[137], R. Mantifel[86], L. Mapelli[30], L. March[168], J.F. Marchand[29], F. Marchese[134a,134b], G. Marchiori[79], M. Marcisovsky[126], C.P. Marino[170], C.N. Marques[125a], F. Marroquim[24a], Z. Marshall[121], L.F. Marti[17], S. Marti-Garcia[168], B. Martin[30], B. Martin[89], J.P. Martin[94], T.A. Martin[171], V.J. Martin[46], B. Martin dit Latour[49], H. Martinez[137], M. Martinez[12,p], S. Martin-Haugh[150], A.C. Martyniuk[170], M. Marx[83], F. Marzano[133a], A. Marzin[112], L. Masetti[82], T. Mashimo[156], R. Mashinistov[95], J. Masik[83], A.L. Maslennikov[108], I. Massa[20a,20b], N. Massol[5], P. Mastrandrea[149], A. Mastroberardino[37a,37b], T. Masubuchi[156], H. Matsunaga[156], T. Matsushita[66], P. Mättig[176], S. Mättig[42], C. Mattravers[119,d], J. Maurer[84], S.J. Maxfield[73], D.A. Maximov[108,g], R. Mazini[152], M. Mazur[21], L. Mazzaferro[134a,134b], M. Mazzanti[90a], S.P. Mc Kee[88], A. McCarn[166], R.L. McCarthy[149], T.G. McCarthy[29], N.A. McCubbin[130], K.W. McFarlane[56,*], J.A. Mcfayden[140], G. Mchedlidze[51b], T. Mclaughlan[18], S.J. McMahon[130], R.A. McPherson[170,j], A. Meade[85], J. Mechnich[106], M. Mechtel[176], M. Medinnis[42], S. Meehan[31], R. Meera-Lebbai[112], T. Meguro[117], S. Mehlhase[36], A. Mehta[73], K. Meier[58a], C. Meineck[99], B. Meirose[80], C. Melachrinos[31], B.R. Mellado Garcia[146c], F. Meloni[90a,90b], L. Mendoza Navas[163], A. Mengarelli[20a,20b], S. Menke[100], E. Meoni[162], K.M. Mercurio[57], N. Meric[137], P. Mermod[49], L. Merola[103a,103b], C. Meroni[90a], F.S. Merritt[31], H. Merritt[110], A. Messina[30,z], J. Metcalfe[25], A.S. Mete[164], C. Meyer[82], C. Meyer[31], J-P. Meyer[137], J. Meyer[30], J. Meyer[54], S. Michal[30], R.P. Middleton[130], S. Migas[73], L. Mijović[137], G. Mikenberg[173], M. Mikestikova[126], M. Mikuž[74], D.W. Miller[31], W.J. Mills[169], C. Mills[57], A. Milov[173], D.A. Milstead[147a,147b], D. Milstein[173], A.A. Minaenko[129], M. Miñano Moya[168], I.A. Minashvili[64], A.I. Mincer[109], B. Mindur[38a], M. Mineev[64], Y. Ming[174], L.M. Mir[12], G. Mirabelli[133a], J. Mitrevski[138], V.A. Mitsou[168], S. Mitsui[65], P.S. Miyagawa[140], J.U. Mjörnmark[80], T. Moa[147a,147b], V. Moeller[28], S. Mohapatra[149], W. Mohr[48], R. Moles-Valls[168],

A. Molfetas[30], K. Mönig[42], C. Monini[55], J. Monk[36], E. Monnier[84], J. Montejo Berlingen[12],
F. Monticelli[70], S. Monzani[20a,20b], R.W. Moore[3], C. Mora Herrera[49], A. Moraes[53], N. Morange[62],
J. Morel[54], D. Moreno[82], M. Moreno Llácer[168], P. Morettini[50a], M. Morgenstern[44], M. Morii[57],
S. Moritz[82], A.K. Morley[30], G. Mornacchi[30], J.D. Morris[75], L. Morvaj[102], N. Möser[21],
H.G. Moser[100], M. Mosidze[51b], J. Moss[110], R. Mount[144], E. Mountricha[10,aa], S.V. Mouraviev[95,*],
E.J.W. Moyse[85], R.D. Mudd[18], F. Mueller[58a], J. Mueller[124], K. Mueller[21], T. Mueller[28],
T. Mueller[82], D. Muenstermann[30], Y. Munwes[154], J.A. Murillo Quijada[18], W.J. Murray[130],
I. Mussche[106], E. Musto[153], A.G. Myagkov[129,ab], M. Myska[126], O. Nackenhorst[54], J. Nadal[12],
K. Nagai[161], R. Nagai[158], Y. Nagai[84], K. Nagano[65], A. Nagarkar[110], Y. Nagasaka[59], M. Nagel[100],
A.M. Nairz[30], Y. Nakahama[30], K. Nakamura[65], T. Nakamura[156], I. Nakano[111], H. Namasivayam[41],
G. Nanava[21], A. Napier[162], R. Narayan[58b], M. Nash[77,d], T. Nattermann[21], T. Naumann[42],
G. Navarro[163], H.A. Neal[88], P.Yu. Nechaeva[95], T.J. Neep[83], A. Negri[120a,120b], G. Negri[30],
M. Negrini[20a], S. Nektarijevic[49], A. Nelson[164], T.K. Nelson[144], S. Nemecek[126], P. Nemethy[109],
A.A. Nepomuceno[24a], M. Nessi[30,ac], M.S. Neubauer[166], M. Neumann[176], A. Neusiedl[82],
R.M. Neves[109], P. Nevski[25], F.M. Newcomer[121], P.R. Newman[18], D.H. Nguyen[6],
V. Nguyen Thi Hong[137], R.B. Nickerson[119], R. Nicolaidou[137], B. Nicquevert[30], F. Niedercorn[116],
J. Nielsen[138], N. Nikiforou[35], A. Nikiforov[16], V. Nikolaenko[129,ab], I. Nikolic-Audit[79],
K. Nikolics[49], K. Nikolopoulos[18], P. Nilsson[8], Y. Ninomiya[156], A. Nisati[133a], R. Nisius[100],
T. Nobe[158], L. Nodulman[6], M. Nomachi[117], I. Nomidis[155], S. Norberg[112], M. Nordberg[30],
J. Novakova[128], M. Nozaki[65], L. Nozka[114], A.-E. Nuncio-Quiroz[21], G. Nunes Hanninger[87],
T. Nunnemann[99], E. Nurse[77], B.J. O'Brien[46], D.C. O'Neil[143], V. O'Shea[53], L.B. Oakes[99],
F.G. Oakham[29,e], H. Oberlack[100], J. Ocariz[79], A. Ochi[66], M.I. Ochoa[77], S. Oda[69], S. Odaka[65],
J. Odier[84], H. Ogren[60], A. Oh[83], S.H. Oh[45], C.C. Ohm[30], T. Ohshima[102], W. Okamura[117],
H. Okawa[25], Y. Okumura[31], T. Okuyama[156], A. Olariu[26a], A.G. Olchevski[64], S.A. Olivares Pino[46],
M. Oliveira[125a,h], D. Oliveira Damazio[25], E. Oliver Garcia[168], D. Olivito[121], A. Olszewski[39],
J. Olszowska[39], A. Onofre[125a,ad], P.U.E. Onyisi[31,ae], C.J. Oram[160a], M.J. Oreglia[31], Y. Oren[154],
D. Orestano[135a,135b], N. Orlando[72a,72b], C. Oropeza Barrera[53], R.S. Orr[159], B. Osculati[50a,50b],
R. Ospanov[121], G. Otero y Garzon[27], J.P. Ottersbach[106], M. Ouchrif[136d], E.A. Ouellette[170],
F. Ould-Saada[118], A. Ouraou[137], Q. Ouyang[33a], A. Ovcharova[15], M. Owen[83], S. Owen[140],
V.E. Ozcan[19a], N. Ozturk[8], K. Pachal[119], A. Pacheco Pages[12], C. Padilla Aranda[12],
S. Pagan Griso[15], E. Paganis[140], C. Pahl[100], F. Paige[25], P. Pais[85], K. Pajchel[118], G. Palacino[160b],
C.P. Paleari[7], S. Palestini[30], D. Pallin[34], A. Palma[125a], J.D. Palmer[18], Y.B. Pan[174],
E. Panagiotopoulou[10], J.G. Panduro Vazquez[76], P. Pani[106], N. Panikashvili[88], S. Panitkin[25],
D. Pantea[26a], A. Papadelis[147a], Th.D. Papadopoulou[10], K. Papageorgiou[155,o], A. Paramonov[6],
D. Paredes Hernandez[34], W. Park[25,af], M.A. Parker[28], F. Parodi[50a,50b], J.A. Parsons[35],
U. Parzefall[48], S. Pashapour[54], E. Pasqualucci[133a], S. Passaggio[50a], A. Passeri[135a],
F. Pastore[135a,135b,*], Fr. Pastore[76], G. Pásztor[49,ag], S. Pataraia[176], N.D. Patel[151], J.R. Pater[83],
S. Patricelli[103a,103b], T. Pauly[30], J. Pearce[170], M. Pedersen[118], S. Pedraza Lopez[168],
M.I. Pedraza Morales[174], S.V. Peleganchuk[108], D. Pelikan[167], H. Peng[33b], B. Penning[31],
A. Penson[35], J. Penwell[60], T. Perez Cavalcanti[42], E. Perez Codina[160a], M.T. Pérez García-Estañ[168],
V. Perez Reale[35], L. Perini[90a,90b], H. Pernegger[30], R. Perrino[72a], P. Perrodo[5], V.D. Peshekhonov[64],
K. Peters[30], R.F.Y. Peters[54,ah], B.A. Petersen[30], J. Petersen[30], T.C. Petersen[36], E. Petit[5],
A. Petridis[147a,147b], C. Petridou[155], E. Petrolo[133a], F. Petrucci[135a,135b], D. Petschull[42], M. Petteni[143],

41

R. Pezoa[32b], A. Phan[87], P.W. Phillips[130], G. Piacquadio[144], E. Pianori[171], A. Picazio[49],
E. Piccaro[75], M. Piccinini[20a,20b], S.M. Piec[42], R. Piegaia[27], D.T. Pignotti[110], J.E. Pilcher[31],
A.D. Pilkington[77], J. Pina[125a,c], M. Pinamonti[165a,165c,ai], A. Pinder[119], J.L. Pinfold[3], A. Pingel[36],
B. Pinto[125a], C. Pizio[90a,90b], M.-A. Pleier[25], V. Pleskot[128], E. Plotnikova[64], P. Plucinski[147a,147b],
S. Poddar[58a], F. Podlyski[34], R. Poettgen[82], L. Poggioli[116], D. Pohl[21], M. Pohl[49], G. Polesello[120a],
A. Policicchio[37a,37b], R. Polifka[159], A. Polini[20a], V. Polychronakos[25], D. Pomeroy[23], K. Pommès[30],
L. Pontecorvo[133a], B.G. Pope[89], G.A. Popeneciu[26b], D.S. Popovic[13a], A. Poppleton[30],
X. Portell Bueso[12], G.E. Pospelov[100], S. Pospisil[127], I.N. Potrap[64], C.J. Potter[150], C.T. Potter[115],
G. Poulard[30], J. Poveda[60], V. Pozdnyakov[64], R. Prabhu[77], P. Pralavorio[84], A. Pranko[15],
S. Prasad[30], R. Pravahan[25], S. Prell[63], K. Pretzl[17], D. Price[60], J. Price[73], L.E. Price[6], D. Prieur[124],
M. Primavera[72a], M. Proissl[46], K. Prokofiev[109], F. Prokoshin[32b], E. Protopapadaki[137],
S. Protopopescu[25], J. Proudfoot[6], X. Prudent[44], M. Przybycien[38a], H. Przysiezniak[5],
S. Psoroulas[21], E. Ptacek[115], E. Pueschel[85], D. Puldon[149], M. Purohit[25,af], P. Puzo[116],
Y. Pylypchenko[62], J. Qian[88], A. Quadt[54], D.R. Quarrie[15], W.B. Quayle[174], D. Quilty[53],
M. Raas[105], V. Radeka[25], V. Radescu[42], P. Radloff[115], F. Ragusa[90a,90b], G. Rahal[179],
S. Rajagopalan[25], M. Rammensee[48], M. Rammes[142], A.S. Randle-Conde[40], K. Randrianarivony[29],
C. Rangel-Smith[79], K. Rao[164], F. Rauscher[99], T.C. Rave[48], T. Ravenscroft[53], M. Raymond[30],
A.L. Read[118], D.M. Rebuzzi[120a,120b], A. Redelbach[175], G. Redlinger[25], R. Reece[121], K. Reeves[41],
A. Reinsch[115], I. Reisinger[43], M. Relich[164], C. Rembser[30], Z.L. Ren[152], A. Renaud[116],
M. Rescigno[133a], S. Resconi[90a], B. Resende[137], P. Reznicek[99], R. Rezvani[94], R. Richter[100],
E. Richter-Was[38b], M. Ridel[79], P. Rieck[16], M. Rijssenbeek[149], A. Rimoldi[120a,120b], L. Rinaldi[20a],
R.R. Rios[40], E. Ritsch[61], I. Riu[12], G. Rivoltella[90a,90b], F. Rizatdinova[113], E. Rizvi[75],
S.H. Robertson[86,j], A. Robichaud-Veronneau[119], D. Robinson[28], J.E.M. Robinson[83], A. Robson[53],
J.G. Rocha de Lima[107], C. Roda[123a,123b], D. Roda Dos Santos[30], A. Roe[54], S. Roe[30], O. Røhne[118],
S. Rolli[162], A. Romaniouk[97], M. Romano[20a,20b], G. Romeo[27], E. Romero Adam[168],
N. Rompotis[139], L. Roos[79], E. Ros[168], S. Rosati[133a], K. Rosbach[49], A. Rose[150], M. Rose[76],
G.A. Rosenbaum[159], P.L. Rosendahl[14], O. Rosenthal[142], V. Rossetti[12], E. Rossi[133a,133b],
L.P. Rossi[50a], M. Rotaru[26a], I. Roth[173], J. Rothberg[139], D. Rousseau[116], C.R. Royon[137],
A. Rozanov[84], Y. Rozen[153], X. Ruan[146c], F. Rubbo[12], I. Rubinskiy[42], N. Ruckstuhl[106], V.I. Rud[98],
C. Rudolph[44], M.S. Rudolph[159], F. Rühr[7], A. Ruiz-Martinez[63], L. Rumyantsev[64], Z. Rurikova[48],
N.A. Rusakovich[64], A. Ruschke[99], J.P. Rutherfoord[7], N. Ruthmann[48], P. Ruzicka[126],
Y.F. Ryabov[122], M. Rybar[128], G. Rybkin[116], N.C. Ryder[119], A.F. Saavedra[151], A. Saddique[3],
I. Sadeh[154], H.F-W. Sadrozinski[138], R. Sadykov[64], F. Safai Tehrani[133a], H. Sakamoto[156],
G. Salamanna[75], A. Salamon[134a], M. Saleem[112], D. Salek[30], D. Salihagic[100], A. Salnikov[144],
J. Salt[168], B.M. Salvachua Ferrando[6], D. Salvatore[37a,37b], F. Salvatore[150], A. Salvucci[105],
A. Salzburger[30], D. Sampsonidis[155], A. Sanchez[103a,103b], J. Sánchez[168], V. Sanchez Martinez[168],
H. Sandaker[14], H.G. Sander[82], M.P. Sanders[99], M. Sandhoff[176], T. Sandoval[28], C. Sandoval[163],
R. Sandstroem[100], D.P.C. Sankey[130], A. Sansoni[47], C. Santoni[34], R. Santonico[134a,134b],
H. Santos[125a], I. Santoyo Castillo[150], K. Sapp[124], J.G. Saraiva[125a], T. Sarangi[174],
E. Sarkisyan-Grinbaum[8], B. Sarrazin[21], F. Sarri[123a,123b], G. Sartisohn[176], O. Sasaki[65], Y. Sasaki[156],
N. Sasao[67], I. Satsounkevitch[91], G. Sauvage[5,*], E. Sauvan[5], J.B. Sauvan[116], P. Savard[159,e],
V. Savinov[124], D.O. Savu[30], C. Sawyer[119], L. Sawyer[78,l], D.H. Saxon[53], J. Saxon[121], C. Sbarra[20a],
A. Sbrizzi[3], D.A. Scannicchio[164], M. Scarcella[151], J. Schaarschmidt[116], P. Schacht[100],

D. Schaefer[121], A. Schaelicke[46], S. Schaepe[21], S. Schaetzel[58b], U. Schäfer[82], A.C. Schaffer[116],
D. Schaile[99], R.D. Schamberger[149], V. Scharf[58a], V.A. Schegelsky[122], D. Scheirich[88],
M. Schernau[164], M.I. Scherzer[35], C. Schiavi[50a,50b], J. Schieck[99], C. Schillo[48], M. Schioppa[37a,37b],
S. Schlenker[30], E. Schmidt[48], K. Schmieden[30], C. Schmitt[82], C. Schmitt[99], S. Schmitt[58b],
B. Schneider[17], Y.J. Schnellbach[73], U. Schnoor[44], L. Schoeffel[137], A. Schoening[58b],
A.L.S. Schorlemmer[54], M. Schott[82], D. Schouten[160a], J. Schovancova[126], M. Schram[86],
C. Schroeder[82], N. Schroer[58c], M.J. Schultens[21], H.-C. Schultz-Coulon[58a], H. Schulz[16],
M. Schumacher[48], B.A. Schumm[138], Ph. Schune[137], A. Schwartzman[144], Ph. Schwegler[100],
Ph. Schwemling[137], R. Schwienhorst[89], J. Schwindling[137], T. Schwindt[21], M. Schwoerer[5],
F.G. Sciacca[17], E. Scifo[116], G. Sciolla[23], W.G. Scott[130], F. Scutti[21], J. Searcy[88], G. Sedov[42],
E. Sedykh[122], S.C. Seidel[104], A. Seiden[138], F. Seifert[44], J.M. Seixas[24a], G. Sekhniaidze[103a],
S.J. Sekula[40], K.E. Selbach[46], D.M. Seliverstov[122], G. Sellers[73], M. Seman[145b],
N. Semprini-Cesari[20a,20b], C. Serfon[30], L. Serin[116], L. Serkin[54], T. Serre[84], R. Seuster[160a],
H. Severini[112], A. Sfyrla[30], E. Shabalina[54], M. Shamim[115], L.Y. Shan[33a], J.T. Shank[22],
Q.T. Shao[87], M. Shapiro[15], P.B. Shatalov[96], K. Shaw[165a,165c], P. Sherwood[77], S. Shimizu[102],
M. Shimojima[101], T. Shin[56], M. Shiyakova[64], A. Shmeleva[95], M.J. Shochet[31], D. Short[119],
S. Shrestha[63], E. Shulga[97], M.A. Shupe[7], P. Sicho[126], A. Sidoti[133a], F. Siegert[48], Dj. Sijacki[13a],
O. Silbert[173], J. Silva[125a], Y. Silver[154], D. Silverstein[144], S.B. Silverstein[147a], V. Simak[127],
O. Simard[5], Lj. Simic[13a], S. Simion[116], E. Simioni[82], B. Simmons[77], R. Simoniello[90a,90b],
M. Simonyan[36], P. Sinervo[159], N.B. Sinev[115], V. Sipica[142], G. Siragusa[175], A. Sircar[78],
A.N. Sisakyan[64,*], S.Yu. Sivoklokov[98], J. Sjölin[147a,147b], T.B. Sjursen[14], L.A. Skinnari[15],
H.P. Skottowe[57], K.Yu. Skovpen[108], P. Skubic[112], M. Slater[18], T. Slavicek[127], K. Sliwa[162],
V. Smakhtin[173], B.H. Smart[46], L. Smestad[118], S.Yu. Smirnov[97], Y. Smirnov[97], L.N. Smirnova[98,aj],
O. Smirnova[80], K.M. Smith[53], M. Smizanska[71], K. Smolek[127], A.A. Snesarev[95], G. Snidero[75],
J. Snow[112], S. Snyder[25], R. Sobie[170,j], J. Sodomka[127], A. Soffer[154], D.A. Soh[152,v], C.A. Solans[30],
M. Solar[127], J. Solc[127], E.Yu. Soldatov[97], U. Soldevila[168], E. Solfaroli Camillocci[133a,133b],
A.A. Solodkov[129], O.V. Solovyanov[129], V. Solovyev[122], N. Soni[1], A. Sood[15], V. Sopko[127],
B. Sopko[127], M. Sosebee[8], R. Soualah[165a,165c], P. Soueid[94], A.M. Soukharev[108], D. South[42],
S. Spagnolo[72a,72b], F. Spanò[76], R. Spighi[20a], G. Spigo[30], R. Spiwoks[30], M. Spousta[128,ak],
T. Spreitzer[159], B. Spurlock[8], R.D. St. Denis[53], J. Stahlman[121], R. Stamen[58a], E. Stanecka[39],
R.W. Stanek[6], C. Stanescu[135a], M. Stanescu-Bellu[42], M.M. Stanitzki[42], S. Stapnes[118],
E.A. Starchenko[129], J. Stark[55], P. Staroba[126], P. Starovoitov[42], R. Staszewski[39], A. Staude[99],
P. Stavina[145a,*], G. Steele[53], P. Steinbach[44], P. Steinberg[25], I. Stekl[127], B. Stelzer[143], H.J. Stelzer[89],
O. Stelzer-Chilton[160a], H. Stenzel[52], S. Stern[100], G.A. Stewart[30], J.A. Stillings[21], M.C. Stockton[86],
M. Stoebe[86], K. Stoerig[48], G. Stoicea[26a], S. Stonjek[100], A.R. Stradling[8], A. Straessner[44],
J. Strandberg[148], S. Strandberg[147a,147b], A. Strandlie[118], M. Strang[110], E. Strauss[144], M. Strauss[112],
P. Strizenec[145b], R. Ströhmer[175], D.M. Strom[115], J.A. Strong[76,*], R. Stroynowski[40], B. Stugu[14],
I. Stumer[25,*], J. Stupak[149], P. Sturm[176], N.A. Styles[42], D. Su[144], HS. Subramania[3],
R. Subramaniam[78], A. Succurro[12], Y. Sugaya[117], C. Suhr[107], M. Suk[127], V.V. Sulin[95],
S. Sultansoy[4c], T. Sumida[67], X. Sun[55], J.E. Sundermann[48], K. Suruliz[140], G. Susinno[37a,37b],
M.R. Sutton[150], Y. Suzuki[65], Y. Suzuki[66], M. Svatos[126], S. Swedish[169], M. Swiatlowski[144],
I. Sykora[145a], T. Sykora[128], D. Ta[106], K. Tackmann[42], A. Taffard[164], R. Tafirout[160a], N. Taiblum[154],
Y. Takahashi[102], H. Takai[25], R. Takashima[68], H. Takeda[66], T. Takeshita[141], Y. Takubo[65],

M. Talby[84], A.A. Talyshev[108,g], J.Y.C. Tam[175], M.C. Tamsett[78,al], K.G. Tan[87], J. Tanaka[156],
R. Tanaka[116], S. Tanaka[132], S. Tanaka[65], A.J. Tanasijczuk[143], K. Tani[66], N. Tannoury[84],
S. Tapprogge[82], S. Tarem[153], F. Tarrade[29], G.F. Tartarelli[90a], P. Tas[128], M. Tasevsky[126],
T. Tashiro[67], E. Tassi[37a,37b], Y. Tayalati[136d], C. Taylor[77], F.E. Taylor[93], G.N. Taylor[87],
W. Taylor[160b], M. Teinturier[116], F.A. Teischinger[30], M. Teixeira Dias Castanheira[75],
P. Teixeira-Dias[76], K.K. Temming[48], H. Ten Kate[30], P.K. Teng[152], S. Terada[65], K. Terashi[156],
J. Terron[81], M. Testa[47], R.J. Teuscher[159,j], J. Therhaag[21], T. Theveneaux-Pelzer[34], S. Thoma[48],
J.P. Thomas[18], E.N. Thompson[35], P.D. Thompson[18], P.D. Thompson[159], A.S. Thompson[53],
L.A. Thomsen[36], E. Thomson[121], M. Thomson[28], W.M. Thong[87], R.P. Thun[88,*], F. Tian[35],
M.J. Tibbetts[15], T. Tic[126], V.O. Tikhomirov[95], Yu.A. Tikhonov[108,g], S. Timoshenko[97],
E. Tiouchichine[84], P. Tipton[177], S. Tisserant[84], T. Todorov[5], S. Todorova-Nova[162],
B. Toggerson[164], J. Tojo[69], S. Tokár[145a], K. Tokushuku[65], K. Tollefson[89], L. Tomlinson[83],
M. Tomoto[102], L. Tompkins[31], K. Toms[104], A. Tonoyan[14], C. Topfel[17], N.D. Topilin[64],
E. Torrence[115], H. Torres[79], E. Torró Pastor[168], J. Toth[84,ag], F. Touchard[84], D.R. Tovey[140],
H.L. Tran[116], T. Trefzger[175], L. Tremblet[30], A. Tricoli[30], I.M. Trigger[160a], S. Trincaz-Duvoid[79],
M.F. Tripiana[70], N. Triplett[25], W. Trischuk[159], B. Trocmé[55], C. Troncon[90a],
M. Trottier-McDonald[143], M. Trovatelli[135a,135b], P. True[89], M. Trzebinski[39], A. Trzupek[39],
C. Tsarouchas[30], J.C-L. Tseng[119], M. Tsiakiris[106], P.V. Tsiareshka[91], D. Tsionou[137],
G. Tsipolitis[10], S. Tsiskaridze[12], V. Tsiskaridze[48], E.G. Tskhadadze[51a], I.I. Tsukerman[96],
V. Tsulaia[15], J.-W. Tsung[21], S. Tsuno[65], D. Tsybychev[149], A. Tua[140], A. Tudorache[26a],
V. Tudorache[26a], J.M. Tuggle[31], A.N. Tuna[121], M. Turala[39], D. Turecek[127], I. Turk Cakir[4d],
R. Turra[90a,90b], P.M. Tuts[35], A. Tykhonov[74], M. Tylmad[147a,147b], M. Tyndel[130], K. Uchida[21],
I. Ueda[156], R. Ueno[29], M. Ughetto[84], M. Ugland[14], M. Uhlenbrock[21], F. Ukegawa[161], G. Unal[30],
A. Undrus[25], G. Unel[164], F.C. Ungaro[48], Y. Unno[65], D. Urbaniec[35], P. Urquijo[21], G. Usai[8],
L. Vacavant[84], V. Vacek[127], B. Vachon[86], S. Vahsen[15], N. Valencic[106], S. Valentinetti[20a,20b],
A. Valero[168], L. Valery[34], S. Valkar[128], E. Valladolid Gallego[168], S. Vallecorsa[153],
J.A. Valls Ferrer[168], R. Van Berg[121], P.C. Van Der Deijl[106], R. van der Geer[106], H. van der Graaf[106],
R. Van Der Leeuw[106], D. van der Ster[30], N. van Eldik[30], P. van Gemmeren[6], J. Van Nieuwkoop[143],
I. van Vulpen[106], M. Vanadia[100], W. Vandelli[30], A. Vaniachine[6], P. Vankov[42], F. Vannucci[79],
R. Vari[133a], E.W. Varnes[7], T. Varol[85], D. Varouchas[15], A. Vartapetian[8], K.E. Varvell[151],
V.I. Vassilakopoulos[56], F. Vazeille[34], T. Vazquez Schroeder[54], F. Veloso[125a], S. Veneziano[133a],
A. Ventura[72a,72b], D. Ventura[85], M. Venturi[48], N. Venturi[159], V. Vercesi[120a], M. Verducci[139],
W. Verkerke[106], J.C. Vermeulen[106], A. Vest[44], M.C. Vetterli[143,e], I. Vichou[166], T. Vickey[146c,am],
O.E. Vickey Boeriu[146c], G.H.A. Viehhauser[119], S. Viel[169], M. Villa[20a,20b], M. Villaplana Perez[168],
E. Vilucchi[47], M.G. Vincter[29], V.B. Vinogradov[64], J. Virzi[15], O. Vitells[173], M. Viti[42], I. Vivarelli[48],
F. Vives Vaque[3], S. Vlachos[10], D. Vladoiu[99], M. Vlasak[127], A. Vogel[21], P. Vokac[127], G. Volpi[47],
M. Volpi[87], G. Volpini[90a], H. von der Schmitt[100], H. von Radziewski[48], E. von Toerne[21],
V. Vorobel[128], M. Vos[168], R. Voss[30], J.H. Vossebeld[73], N. Vranjes[137], M. Vranjes Milosavljevic[106],
V. Vrba[126], M. Vreeswijk[106], T. Vu Anh[48], R. Vuillermet[30], I. Vukotic[31], Z. Vykydal[127],
W. Wagner[176], P. Wagner[21], S. Wahrmund[44], J. Wakabayashi[102], S. Walch[88], J. Walder[71],
R. Walker[99], W. Walkowiak[142], R. Wall[177], P. Waller[73], B. Walsh[177], C. Wang[45], H. Wang[174],
H. Wang[40], J. Wang[152], J. Wang[33a], K. Wang[86], R. Wang[104], S.M. Wang[152], T. Wang[21],
X. Wang[177], A. Warburton[86], C.P. Ward[28], D.R. Wardrope[77], M. Warsinsky[48], A. Washbrook[46],

44

C. Wasicki[42], I. Watanabe[66], P.M. Watkins[18], A.T. Watson[18], I.J. Watson[151], M.F. Watson[18], G. Watts[139], S. Watts[83], A.T. Waugh[151], B.M. Waugh[77], M.S. Weber[17], J.S. Webster[31], A.R. Weidberg[119], P. Weigell[100], J. Weingarten[54], C. Weiser[48], P.S. Wells[30], T. Wenaus[25], D. Wendland[16], Z. Weng[152,v], T. Wengler[30], S. Wenig[30], N. Wermes[21], M. Werner[48], P. Werner[30], M. Werth[164], M. Wessels[58a], J. Wetter[162], K. Whalen[29], A. White[8], M.J. White[87], R. White[32b], S. White[123a,123b], S.R. Whitehead[119], D. Whiteson[164], D. Whittington[60], D. Wicke[176], F.J. Wickens[130], W. Wiedenmann[174], M. Wielers[80,d], P. Wienemann[21], C. Wiglesworth[36], L.A.M. Wiik-Fuchs[21], P.A. Wijeratne[77], A. Wildauer[100], M.A. Wildt[42,s], I. Wilhelm[128], H.G. Wilkens[30], J.Z. Will[99], E. Williams[35], H.H. Williams[121], S. Williams[28], W. Willis[35,*], S. Willocq[85], J.A. Wilson[18], A. Wilson[88], I. Wingerter-Seez[5], S. Winkelmann[48], F. Winklmeier[30], M. Wittgen[144], T. Wittig[43], J. Wittkowski[99], S.J. Wollstadt[82], M.W. Wolter[39], H. Wolters[125a,h], W.C. Wong[41], G. Wooden[88], B.K. Wosiek[39], J. Wotschack[30], M.J. Woudstra[83], K.W. Wozniak[39], K. Wraight[53], M. Wright[53], B. Wrona[73], S.L. Wu[174], X. Wu[49], Y. Wu[88], E. Wulf[35], B.M. Wynne[46], S. Xella[36], M. Xiao[137], S. Xie[48], C. Xu[33b,aa], D. Xu[33a], L. Xu[33b,an], B. Yabsley[151], S. Yacoob[146b,ao], M. Yamada[65], H. Yamaguchi[156], Y. Yamaguchi[156], A. Yamamoto[65], K. Yamamoto[63], S. Yamamoto[156], T. Yamamura[156], T. Yamanaka[156], K. Yamauchi[102], T. Yamazaki[156], Y. Yamazaki[66], Z. Yan[22], H. Yang[33e], H. Yang[174], U.K. Yang[83], Y. Yang[110], Z. Yang[147a,147b], S. Yanush[92], L. Yao[33a], Y. Yasu[65], E. Yatsenko[42], K.H. Yau Wong[21], J. Ye[40], S. Ye[25], A.L. Yen[57], E. Yildirim[42], M. Yilmaz[4b], R. Yoosoofmiya[124], K. Yorita[172], R. Yoshida[6], K. Yoshihara[156], C. Young[144], C.J.S. Young[119], S. Youssef[22], D. Yu[25], D.R. Yu[15], J. Yu[8], J. Yu[113], L. Yuan[66], A. Yurkewicz[107], B. Zabinski[39], R. Zaidan[62], A.M. Zaitsev[129,ab], S. Zambito[23], L. Zanello[133a,133b], D. Zanzi[100], A. Zaytsev[25], C. Zeitnitz[176], M. Zeman[127], A. Zemla[39], O. Zenin[129], T. Ženiš[145a], D. Zerwas[116], G. Zevi della Porta[57], D. Zhang[88], H. Zhang[89], J. Zhang[6], L. Zhang[152], X. Zhang[33d], Z. Zhang[116], Z. Zhao[33b], A. Zhemchugov[64], J. Zhong[119], B. Zhou[88], N. Zhou[164], Y. Zhou[152], C.G. Zhu[33d], H. Zhu[42], J. Zhu[88], Y. Zhu[33b], X. Zhuang[33a], A. Zibell[99], D. Zieminska[60], N.I. Zimin[64], C. Zimmermann[82], R. Zimmermann[21], S. Zimmermann[21], S. Zimmermann[48], Z. Zinonos[123a,123b], M. Ziolkowski[142], R. Zitoun[5], L. Živković[35], V.V. Zmouchko[129,*], G. Zobernig[174], A. Zoccoli[20a,20b], M. zur Nedden[16], V. Zutshi[107], L. Zwalinski[30].

[1] School of Chemistry and Physics, University of Adelaide, Adelaide, Australia

[2] Physics Department, SUNY Albany, Albany NY, United States of America

[3] Department of Physics, University of Alberta, Edmonton AB, Canada

[4] (a) Department of Physics, Ankara University, Ankara; (b) Department of Physics, Gazi University, Ankara; (c) Division of Physics, TOBB University of Economics and Technology, Ankara; (d) Turkish Atomic Energy Authority, Ankara, Turkey

[5] LAPP, CNRS/IN2P3 and Université de Savoie, Annecy-le-Vieux, France

[6] High Energy Physics Division, Argonne National Laboratory, Argonne IL, United States of America

[7] Department of Physics, University of Arizona, Tucson AZ, United States of America

[8] Department of Physics, The University of Texas at Arlington, Arlington TX, United States of America

[9] Physics Department, University of Athens, Athens, Greece

[10] Physics Department, National Technical University of Athens, Zografou, Greece

[11] Institute of Physics, Azerbaijan Academy of Sciences, Baku, Azerbaijan

[12] Institut de Física d'Altes Energies and Departament de Física de la Universitat Autònoma de Barcelona, Barcelona, Spain

[13] [a] Institute of Physics, University of Belgrade, Belgrade; [b] Vinca Institute of Nuclear Sciences, University of Belgrade, Belgrade, Serbia

[14] Department for Physics and Technology, University of Bergen, Bergen, Norway

[15] Physics Division, Lawrence Berkeley National Laboratory and University of California, Berkeley CA, United States of America

[16] Department of Physics, Humboldt University, Berlin, Germany

[17] Albert Einstein Center for Fundamental Physics and Laboratory for High Energy Physics, University of Bern, Bern, Switzerland

[18] School of Physics and Astronomy, University of Birmingham, Birmingham, United Kingdom

[19] [a] Department of Physics, Bogazici University, Istanbul; [b] Department of Physics, Dogus University, Istanbul; [c] Department of Physics Engineering, Gaziantep University, Gaziantep, Turkey

[20] [a] INFN Sezione di Bologna; [b] Dipartimento di Fisica e Astronomia, Università di Bologna, Bologna, Italy

[21] Physikalisches Institut, University of Bonn, Bonn, Germany

[22] Department of Physics, Boston University, Boston MA, United States of America

[23] Department of Physics, Brandeis University, Waltham MA, United States of America

[24] [a] Universidade Federal do Rio De Janeiro COPPE/EE/IF, Rio de Janeiro; [b] Federal University of Juiz de Fora (UFJF), Juiz de Fora; [c] Federal University of Sao Joao del Rei (UFSJ), Sao Joao del Rei; [d] Instituto de Fisica, Universidade de Sao Paulo, Sao Paulo, Brazil

[25] Physics Department, Brookhaven National Laboratory, Upton NY, United States of America

[26] [a] National Institute of Physics and Nuclear Engineering, Bucharest; [b] National Institute for Research and Development of Isotopic and Molecular Technologies, Physics Department, Cluj Napoca; [c] University Politehnica Bucharest, Bucharest; [d] West University in Timisoara, Timisoara, Romania

[27] Departamento de Física, Universidad de Buenos Aires, Buenos Aires, Argentina

[28] Cavendish Laboratory, University of Cambridge, Cambridge, United Kingdom

[29] Department of Physics, Carleton University, Ottawa ON, Canada

[30] CERN, Geneva, Switzerland

[31] Enrico Fermi Institute, University of Chicago, Chicago IL, United States of America

[32] [a] Departamento de Física, Pontificia Universidad Católica de Chile, Santiago; [b] Departamento de Física, Universidad Técnica Federico Santa María, Valparaíso, Chile

[33] [a] Institute of High Energy Physics, Chinese Academy of Sciences, Beijing; [b] Department of Modern Physics, University of Science and Technology of China, Anhui; [c] Department of Physics, Nanjing University, Jiangsu; [d] School of Physics, Shandong University, Shandong; [e] Physics Department, Shanghai Jiao Tong University, Shanghai, China

[34] Laboratoire de Physique Corpusculaire, Clermont Université and Université Blaise Pascal and CNRS/IN2P3, Clermont-Ferrand, France

[35] Nevis Laboratory, Columbia University, Irvington NY, United States of America

[36] Niels Bohr Institute, University of Copenhagen, Kobenhavn, Denmark

[37] [a] INFN Gruppo Collegato di Cosenza; [b] Dipartimento di Fisica, Università della Calabria, Rende, Italy

[38] [a] AGH University of Science and Technology, Faculty of Physics and Applied Computer Science, Krakow; [b] Marian Smoluchowski Institute of Physics, Jagiellonian University, Krakow, Poland

[39] The Henryk Niewodniczanski Institute of Nuclear Physics, Polish Academy of Sciences, Krakow, Poland

[40] Physics Department, Southern Methodist University, Dallas TX, United States of America

[41] Physics Department, University of Texas at Dallas, Richardson TX, United States of America

[42] DESY, Hamburg and Zeuthen, Germany

[43] Institut für Experimentelle Physik IV, Technische Universität Dortmund, Dortmund, Germany

[44] Institut für Kern- und Teilchenphysik, Technische Universität Dresden, Dresden, Germany

[45] Department of Physics, Duke University, Durham NC, United States of America

[46] SUPA - School of Physics and Astronomy, University of Edinburgh, Edinburgh, United Kingdom

[47] INFN Laboratori Nazionali di Frascati, Frascati, Italy

[48] Fakultät für Mathematik und Physik, Albert-Ludwigs-Universität, Freiburg, Germany

[49] Section de Physique, Université de Genève, Geneva, Switzerland

[50] [a] INFN Sezione di Genova; [b] Dipartimento di Fisica, Università di Genova, Genova, Italy

[51] [a] E. Andronikashvili Institute of Physics, Iv. Javakhishvili Tbilisi State University, Tbilisi; [b] High Energy Physics Institute, Tbilisi State University, Tbilisi, Georgia

[52] II Physikalisches Institut, Justus-Liebig-Universität Giessen, Giessen, Germany

[53] SUPA - School of Physics and Astronomy, University of Glasgow, Glasgow, United Kingdom

[54] II Physikalisches Institut, Georg-August-Universität, Göttingen, Germany

[55] Laboratoire de Physique Subatomique et de Cosmologie, Université Joseph Fourier and CNRS/IN2P3 and Institut National Polytechnique de Grenoble, Grenoble, France

[56] Department of Physics, Hampton University, Hampton VA, United States of America

[57] Laboratory for Particle Physics and Cosmology, Harvard University, Cambridge MA, United States of America

[58] [a] Kirchhoff-Institut für Physik, Ruprecht-Karls-Universität Heidelberg, Heidelberg; [b] Physikalisches Institut, Ruprecht-Karls-Universität Heidelberg, Heidelberg; [c] ZITI Institut für technische Informatik, Ruprecht-Karls-Universität Heidelberg, Mannheim, Germany

[59] Faculty of Applied Information Science, Hiroshima Institute of Technology, Hiroshima, Japan

[60] Department of Physics, Indiana University, Bloomington IN, United States of America

[61] Institut für Astro- und Teilchenphysik, Leopold-Franzens-Universität, Innsbruck, Austria

[62] University of Iowa, Iowa City IA, United States of America

[63] Department of Physics and Astronomy, Iowa State University, Ames IA, United States of America

[64] Joint Institute for Nuclear Research, JINR Dubna, Dubna, Russia

[65] KEK, High Energy Accelerator Research Organization, Tsukuba, Japan

[66] Graduate School of Science, Kobe University, Kobe, Japan

[67] Faculty of Science, Kyoto University, Kyoto, Japan

[68] Kyoto University of Education, Kyoto, Japan

[69] Department of Physics, Kyushu University, Fukuoka, Japan

[70] Instituto de Física La Plata, Universidad Nacional de La Plata and CONICET, La Plata, Argentina

[71] Physics Department, Lancaster University, Lancaster, United Kingdom

[72] [a] INFN Sezione di Lecce; [b] Dipartimento di Matematica e Fisica, Università del Salento, Lecce, Italy

[73] Oliver Lodge Laboratory, University of Liverpool, Liverpool, United Kingdom

[74] Department of Physics, Jožef Stefan Institute and University of Ljubljana, Ljubljana, Slovenia

[75] School of Physics and Astronomy, Queen Mary University of London, London, United Kingdom

[76] Department of Physics, Royal Holloway University of London, Surrey, United Kingdom

[77] Department of Physics and Astronomy, University College London, London, United Kingdom

[78] Louisiana Tech University, Ruston LA, United States of America

[79] Laboratoire de Physique Nucléaire et de Hautes Energies, UPMC and Université Paris-Diderot and CNRS/IN2P3, Paris, France

[80] Fysiska institutionen, Lunds universitet, Lund, Sweden

[81] Departamento de Fisica Teorica C-15, Universidad Autonoma de Madrid, Madrid, Spain

[82] Institut für Physik, Universität Mainz, Mainz, Germany

[83] School of Physics and Astronomy, University of Manchester, Manchester, United Kingdom

[84] CPPM, Aix-Marseille Université and CNRS/IN2P3, Marseille, France

[85] Department of Physics, University of Massachusetts, Amherst MA, United States of America

[86] Department of Physics, McGill University, Montreal QC, Canada

[87] School of Physics, University of Melbourne, Victoria, Australia

[88] Department of Physics, The University of Michigan, Ann Arbor MI, United States of America

[89] Department of Physics and Astronomy, Michigan State University, East Lansing MI, United States of America

[90] [a] INFN Sezione di Milano; [b] Dipartimento di Fisica, Università di Milano, Milano, Italy

[91] B.I. Stepanov Institute of Physics, National Academy of Sciences of Belarus, Minsk, Republic of Belarus

[92] National Scientific and Educational Centre for Particle and High Energy Physics, Minsk, Republic of Belarus

[93] Department of Physics, Massachusetts Institute of Technology, Cambridge MA, United States of America

[94] Group of Particle Physics, University of Montreal, Montreal QC, Canada

[95] P.N. Lebedev Institute of Physics, Academy of Sciences, Moscow, Russia

[96] Institute for Theoretical and Experimental Physics (ITEP), Moscow, Russia

[97] Moscow Engineering and Physics Institute (MEPhI), Moscow, Russia

[98] D.V.Skobeltsyn Institute of Nuclear Physics, M.V.Lomonosov Moscow State University, Moscow, Russia

[99] Fakultät für Physik, Ludwig-Maximilians-Universität München, München, Germany

[100] Max-Planck-Institut für Physik (Werner-Heisenberg-Institut), München, Germany

[101] Nagasaki Institute of Applied Science, Nagasaki, Japan

[102] Graduate School of Science and Kobayashi-Maskawa Institute, Nagoya University, Nagoya,

Japan

[103] [a] INFN Sezione di Napoli; [b] Dipartimento di Scienze Fisiche, Università di Napoli, Napoli, Italy

[104] Department of Physics and Astronomy, University of New Mexico, Albuquerque NM, United States of America

[105] Institute for Mathematics, Astrophysics and Particle Physics, Radboud University Nijmegen/Nikhef, Nijmegen, Netherlands

[106] Nikhef National Institute for Subatomic Physics and University of Amsterdam, Amsterdam, Netherlands

[107] Department of Physics, Northern Illinois University, DeKalb IL, United States of America

[108] Budker Institute of Nuclear Physics, SB RAS, Novosibirsk, Russia

[109] Department of Physics, New York University, New York NY, United States of America

[110] Ohio State University, Columbus OH, United States of America

[111] Faculty of Science, Okayama University, Okayama, Japan

[112] Homer L. Dodge Department of Physics and Astronomy, University of Oklahoma, Norman OK, United States of America

[113] Department of Physics, Oklahoma State University, Stillwater OK, United States of America

[114] Palacký University, RCPTM, Olomouc, Czech Republic

[115] Center for High Energy Physics, University of Oregon, Eugene OR, United States of America

[116] LAL, Université Paris-Sud and CNRS/IN2P3, Orsay, France

[117] Graduate School of Science, Osaka University, Osaka, Japan

[118] Department of Physics, University of Oslo, Oslo, Norway

[119] Department of Physics, Oxford University, Oxford, United Kingdom

[120] [a] INFN Sezione di Pavia; [b] Dipartimento di Fisica, Università di Pavia, Pavia, Italy

[121] Department of Physics, University of Pennsylvania, Philadelphia PA, United States of America

[122] Petersburg Nuclear Physics Institute, Gatchina, Russia

[123] [a] INFN Sezione di Pisa; [b] Dipartimento di Fisica E. Fermi, Università di Pisa, Pisa, Italy

[124] Department of Physics and Astronomy, University of Pittsburgh, Pittsburgh PA, United States of America

[125] [a] Laboratorio de Instrumentacao e Fisica Experimental de Particulas - LIP, Lisboa, Portugal; [b] Departamento de Fisica Teorica y del Cosmos and CAFPE, Universidad de Granada, Granada, Spain

[126] Institute of Physics, Academy of Sciences of the Czech Republic, Praha, Czech Republic

[127] Czech Technical University in Prague, Praha, Czech Republic

[128] Faculty of Mathematics and Physics, Charles University in Prague, Praha, Czech Republic

[129] State Research Center Institute for High Energy Physics, Protvino, Russia

[130] Particle Physics Department, Rutherford Appleton Laboratory, Didcot, United Kingdom

[131] Physics Department, University of Regina, Regina SK, Canada

[132] Ritsumeikan University, Kusatsu, Shiga, Japan

[133] [a] INFN Sezione di Roma I; [b] Dipartimento di Fisica, Università La Sapienza, Roma, Italy

[134] [a] INFN Sezione di Roma Tor Vergata; [b] Dipartimento di Fisica, Università di Roma Tor Vergata, Roma, Italy

[135] [a] INFN Sezione di Roma Tre; [b] Dipartimento di Matematica e Fisica, Università Roma Tre, Roma, Italy

[136] [a] Faculté des Sciences Ain Chock, Réseau Universitaire de Physique des Hautes Energies - Université Hassan II, Casablanca; [b] Centre National de l'Energie des Sciences Techniques Nucleaires, Rabat; [c] Faculté des Sciences Semlalia, Université Cadi Ayyad, LPHEA-Marrakech; [d] Faculté des Sciences, Université Mohamed Premier and LPTPM, Oujda; [e] Faculté des sciences, Université Mohammed V-Agdal, Rabat, Morocco

[137] DSM/IRFU (Institut de Recherches sur les Lois Fondamentales de l'Univers), CEA Saclay (Commissariat à l'Energie Atomique et aux Energies Alternatives), Gif-sur-Yvette, France

[138] Santa Cruz Institute for Particle Physics, University of California Santa Cruz, Santa Cruz CA, United States of America

[139] Department of Physics, University of Washington, Seattle WA, United States of America

[140] Department of Physics and Astronomy, University of Sheffield, Sheffield, United Kingdom

[141] Department of Physics, Shinshu University, Nagano, Japan

[142] Fachbereich Physik, Universität Siegen, Siegen, Germany

[143] Department of Physics, Simon Fraser University, Burnaby BC, Canada

[144] SLAC National Accelerator Laboratory, Stanford CA, United States of America

[145] [a] Faculty of Mathematics, Physics & Informatics, Comenius University, Bratislava; [b] Department of Subnuclear Physics, Institute of Experimental Physics of the Slovak Academy of Sciences, Kosice, Slovak Republic

[146] [a] Department of Physics, University of Cape Town, Cape Town; [b] Department of Physics, University of Johannesburg, Johannesburg; [c] School of Physics, University of the Witwatersrand, Johannesburg, South Africa

[147] [a] Department of Physics, Stockholm University; [b] The Oskar Klein Centre, Stockholm, Sweden

[148] Physics Department, Royal Institute of Technology, Stockholm, Sweden

[149] Departments of Physics & Astronomy and Chemistry, Stony Brook University, Stony Brook NY, United States of America

[150] Department of Physics and Astronomy, University of Sussex, Brighton, United Kingdom

[151] School of Physics, University of Sydney, Sydney, Australia

[152] Institute of Physics, Academia Sinica, Taipei, Taiwan

[153] Department of Physics, Technion: Israel Institute of Technology, Haifa, Israel

[154] Raymond and Beverly Sackler School of Physics and Astronomy, Tel Aviv University, Tel Aviv, Israel

[155] Department of Physics, Aristotle University of Thessaloniki, Thessaloniki, Greece

[156] International Center for Elementary Particle Physics and Department of Physics, The University of Tokyo, Tokyo, Japan

[157] Graduate School of Science and Technology, Tokyo Metropolitan University, Tokyo, Japan

[158] Department of Physics, Tokyo Institute of Technology, Tokyo, Japan

[159] Department of Physics, University of Toronto, Toronto ON, Canada

[160] [a] TRIUMF, Vancouver BC; [b] Department of Physics and Astronomy, York University, Toronto ON, Canada

[161] Faculty of Pure and Applied Sciences, University of Tsukuba, Tsukuba, Japan

[162] Department of Physics and Astronomy, Tufts University, Medford MA, United States of America

[163] Centro de Investigaciones, Universidad Antonio Narino, Bogota, Colombia

[164] Department of Physics and Astronomy, University of California Irvine, Irvine CA, United States of America

[165] [a] INFN Gruppo Collegato di Udine; [b] ICTP, Trieste; [c] Dipartimento di Chimica, Fisica e Ambiente, Università di Udine, Udine, Italy

[166] Department of Physics, University of Illinois, Urbana IL, United States of America

[167] Department of Physics and Astronomy, University of Uppsala, Uppsala, Sweden

[168] Instituto de Física Corpuscular (IFIC) and Departamento de Física Atómica, Molecular y Nuclear and Departamento de Ingeniería Electrónica and Instituto de Microelectrónica de Barcelona (IMB-CNM), University of Valencia and CSIC, Valencia, Spain

[169] Department of Physics, University of British Columbia, Vancouver BC, Canada

[170] Department of Physics and Astronomy, University of Victoria, Victoria BC, Canada

[171] Department of Physics, University of Warwick, Coventry, United Kingdom

[172] Waseda University, Tokyo, Japan

[173] Department of Particle Physics, The Weizmann Institute of Science, Rehovot, Israel

[174] Department of Physics, University of Wisconsin, Madison WI, United States of America

[175] Fakultät für Physik und Astronomie, Julius-Maximilians-Universität, Würzburg, Germany

[176] Fachbereich C Physik, Bergische Universität Wuppertal, Wuppertal, Germany

[177] Department of Physics, Yale University, New Haven CT, United States of America

[178] Yerevan Physics Institute, Yerevan, Armenia

[179] Centre de Calcul de l'Institut National de Physique Nucléaire et de Physique des Particules (IN2P3), Villeurbanne, France

[a] Also at Department of Physics, King's College London, London, United Kingdom

[b] Also at Laboratorio de Instrumentacao e Fisica Experimental de Particulas - LIP, Lisboa, Portugal

[c] Also at Faculdade de Ciencias and CFNUL, Universidade de Lisboa, Lisboa, Portugal

[d] Also at Particle Physics Department, Rutherford Appleton Laboratory, Didcot, United Kingdom

[e] Also at TRIUMF, Vancouver BC, Canada

[f] Also at Department of Physics, California State University, Fresno CA, United States of America

[g] Also at Novosibirsk State University, Novosibirsk, Russia

[h] Also at Department of Physics, University of Coimbra, Coimbra, Portugal

[i] Also at Università di Napoli Parthenope, Napoli, Italy

[j] Also at Institute of Particle Physics (IPP), Canada

[k] Also at Department of Physics, Middle East Technical University, Ankara, Turkey

[l] Also at Louisiana Tech University, Ruston LA, United States of America

[m] Also at Dep Fisica and CEFITEC of Faculdade de Ciencias e Tecnologia, Universidade Nova de Lisboa, Caparica, Portugal

[n] Also at Department of Physics and Astronomy, Michigan State University, East Lansing MI, United States of America

[o] Also at Department of Financial and Management Engineering, University of the Aegean,

Chios, Greece

[p] Also at Institucio Catalana de Recerca i Estudis Avancats, ICREA, Barcelona, Spain

[q] Also at Department of Physics, University of Cape Town, Cape Town, South Africa

[r] Also at Institute of Physics, Azerbaijan Academy of Sciences, Baku, Azerbaijan

[s] Also at Institut für Experimentalphysik, Universität Hamburg, Hamburg, Germany

[t] Also at Manhattan College, New York NY, United States of America

[u] Also at Institute of Physics, Academia Sinica, Taipei, Taiwan

[v] Also at School of Physics and Engineering, Sun Yat-sen University, Guanzhou, China

[w] Also at Academia Sinica Grid Computing, Institute of Physics, Academia Sinica, Taipei, Taiwan

[x] Also at Laboratoire de Physique Nucléaire et de Hautes Energies, UPMC and Université Paris-Diderot and CNRS/IN2P3, Paris, France

[y] Also at School of Physical Sciences, National Institute of Science Education and Research, Bhubaneswar, India

[z] Also at Dipartimento di Fisica, Università La Sapienza, Roma, Italy

[aa] Also at DSM/IRFU (Institut de Recherches sur les Lois Fondamentales de l'Univers), CEA Saclay (Commissariat à l'Energie Atomique et aux Energies Alternatives), Gif-sur-Yvette, France

[ab] Also at Moscow Institute of Physics and Technology State University, Dolgoprudny, Russia

[ac] Also at Section de Physique, Université de Genève, Geneva, Switzerland

[ad] Also at Departamento de Fisica, Universidade de Minho, Braga, Portugal

[ae] Also at Department of Physics, The University of Texas at Austin, Austin TX, United States of America

[af] Also at Department of Physics and Astronomy, University of South Carolina, Columbia SC, United States of America

[ag] Also at Institute for Particle and Nuclear Physics, Wigner Research Centre for Physics, Budapest, Hungary

[ah] Also at DESY, Hamburg and Zeuthen, Germany

[ai] Also at International School for Advanced Studies (SISSA), Trieste, Italy

[aj] Also at Faculty of Physics, M.V.Lomonosov Moscow State University, Moscow, Russia

[ak] Also at Nevis Laboratory, Columbia University, Irvington NY, United States of America

[al] Also at Physics Department, Brookhaven National Laboratory, Upton NY, United States of America

[am] Also at Department of Physics, Oxford University, Oxford, United Kingdom

[an] Also at Department of Physics, The University of Michigan, Ann Arbor MI, United States of America

[ao] Also at Discipline of Physics, University of KwaZulu-Natal, Durban, South Africa

[*] Deceased